Magnetic Molecular Conductors

ARTICLE *in* CHEMICAL REVIEWS · NOVEMBER 2004

Impact Factor: 46.57 · DOI: 10.1021/cr030641n · Source: PubMed

2 AUTHORS:

Eugenio Coronado
University of Valencia
610 PUBLICATIONS **18,741** CITATIONS
SEE PROFILE

Peter Day
University College London
639 PUBLICATIONS **11,303** CITATIONS
SEE PROFILE

Magnetic Molecular Conductors

Eugenio Coronado*,† and Peter Day*,‡

Institut de Ciència Molecular de la Universitat de Valencia, C/Doctor Moliner 50, 46100 Burjassot, Spain, and Davy Faraday Research Laboratory, The Royal Institution of Great Britain, 21 Albemarle Street, London W1S 4BS, U.K.

Received March 16, 2004

Contents

1. Introduction

Building multifunctionality in a material is a hot focus of research in contemporary materials science. In this respect molecular chemistry provides unique possibilities, as it allows us to design novel materials that combine in the same crystal lattice two or more physical properties which are difficult or impossible to achieve in continuous lattice solids. A possible approach to reach this goal consists of building up hybrid solids formed by two molecular networks, such as anion/cation salts, where each network furnishes distinct properties to the solid. This approach can give rise to the development of materials with coexistence of properties, or to materials exhibiting novel properties due to the mutual interaction between the two individual networks. Among these hybrid materials, the magnetic molecular conductors mixing magnetism with conductivity (or even superconductivity) have been the most extensively investigated. In this review we report the main achievements obtained in this novel area of research.

Planar organic donors and acceptors such as derivatives of TTF and TCNQ, respectively, have been widely used to synthesize molecular conductors and superconductors. In one of the earliest examples, when TTF reacts with TCNQ, there is a partial electron transfer from the donor to the acceptor to form the charge-transfer salt $[TTF]^{\delta+}[TCNQ]^{\delta-}$, which behaves as a metal. Its structure consists of uniform segregated chains of donor and acceptor molecules, which pack together in the solid state to give delocalized electron energy bands due to overlap between the π orbitals of adjacent molecules. Electron delocalization is also found in solids formed by the ion-radicals resulting from oxidation (or reduction) of one of these two kinds of molecules and a charge-compensating counterion. Such cation-radical salts of organic donors, formulated as $[donor]_mX_n$, have given the most widely studied examples of molecular conductors and superconductors. Typically, the counterion X is a simple inorganic monoanion of the type Cl^-, Br^-, I_3^-, PF_6^-, AsF_6^-, BF_4^-, ClO_4^-, NO_3^-, ...; the structures of these salts consist of segregated stacks of the planar radical cations interleaved by the inorganic anions (Figure 1). A straightforward way

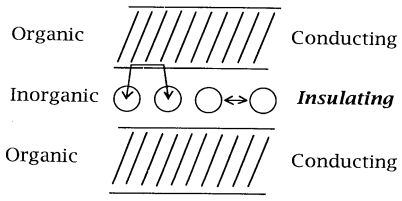

Figure 1. Schematic arrangement of an organic–inorganic composite compound.

of incorporating localized magnetic moments into this class of materials is to use magnetic anions as charge-compensating counterions.

Inorganic chemistry provides a wide choice of metal complexes of various nuclearities and dimensionalities that can be used as charge-compensating counterions of the conducting cation-radical salts. They range from simple mononuclear complexes of the type $[MX_4]^{n-}$ (M = Fe(III), Cu(II); X = Cl, Br), $[M(C_2O_4)_3]^{3-}$ (M = Fe(III), Cr(III)), or $[M(CN)_6]^{3-}$ (M = Fe(III)) to cluster-type complexes (polyoxometalates), to chain complexes such as the substituted dithiolates $[M(mnt)_2]^-$ (mnt = maleonitriledithiolate; M = Ni, Pt, and Pd), to layered structures such as the bimetallic oxalate complexes $[M(II)M(III)(C_2O_4)_3]^-$ (M(II) = Mn, Co, Ni, Fe, Cu; M(III) = Fe, Cr). Most of the examples so far reported of hybrid molecular materials combining a conducting component with a magnetic component are based on the above organic/inorganic combination.[1,2] In this review we concen-

† Institut de Ciència Molecular de la Universitat de Valencia.
‡ The Royal Institution of Great Britain.

10.1021/cr030641n CCC: $48.50
Published on Web 10/22/2004

Eugenio Coronado, born in Valencia in 1959, has been Professor of Inorganic Chemistry at the University of Valencia since 1993 and Director of the University's Institute of Molecular Science (ICMol) since its foundation in 2000. His research interests focus on the chemistry and physics of functional molecular materials, with particular emphasis on their magnetic and electrical properties. In the past few years his main efforts have been devoted to the search for hybrid organic/inorganic molecular materials with multifunctional properties. He is author of more than 280 papers and has edited two books, one on Molecular Magnetism (1996) and the other on Polyoxometalate Molecular Science (2003).

Peter Day earned his first degree and D.Phil. in Inorganic Chemistry from Oxford University, where he was subsequently Departmental Demonstrator, University Lecturer and ad hominem Professor of Solid State Chemistry, and a Fellow of St. John's College. From 1988 to 1991 he was Director of the Institut Laue-Langevin, Grenoble, the European neutron scattering center, and from 1991 to 1998 he was Director of the Royal Institution in London and its Davy-Faraday Research Laboratory, where he remains Fullerian Professor of Chemistry. He was elected FRS in 1986, and in addition to numerous awards from the Royal Society of Chemistry and the Royal Society, he holds honorary Doctorates from the Universities of Newcastle and Kent, and Honorary Fellowships of St. John's and Wadham Colleges, Oxford, and University College, London. His research interests have long centered on the synthesis and electronic properties of molecular organic and metal-organic solids.

trate especially on the structures and properties of cation-radical salts with transition metal-containing anions. Before doing so, however, we summarize some of the reasons that justify the intense effort devoted to this kind of molecular material.

From a physical point of view hybrid materials formed by two molecular networks are interesting because they can permit the coexistence of distinct physical properties originating in each network, or novel and improved properties with respect to those of the two networks alone, due to the interactions between them. In the particular case of materials combining magnetic and conducting properties, an important instance of coexistence that can be sought is that between ferromagnetism and superconductivity. These two collective properties have long been considered as mutually exclusive. Their coexistence has been the subject of lengthy debate between solid-state physicists and has been investigated from both theoretical and experimental points of view in extended inorganic lattices.[3] A second reason for examining the interplay of the localized moments normally found in molecular-based magnetic materials with conduction electrons lies in the possibility of electronic interactions between π and d electrons. Such interactions could play a significant part in stabilizing superconductivity in molecular-based magnetic materials, and in exchange coupling between the magnetic moments through the itinerant electrons of the conducting sublattice (RKKY interaction).[4]

Over the last 15 years there have been many attempts to introduce magnetic centers into conducting molecular lattices by synthesizing charge-transfer salts with transition metal complexes as anions. Because of the great diversity of metals, ligands, connectivity, and structure types, it is difficult to present a unified picture of what has been accomplished, but since the primary interest in the present review concerns the transport properties of molecular charge-transfer salts, the following sections are organized as (a) magnetic superconductors, (b) magnetic conductors and semiconductors, (c) ferromagnetic conductors, and (d) ferrimagnetic insulators. The different organic donors used to form such hybrid organic/inorganic materials are summarized in Chart 1.

Chart 1

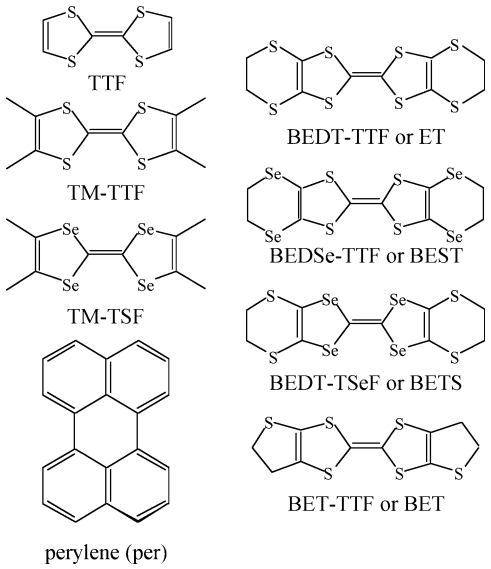

2. Magnetic Superconductors

The fundamental difference between superconductivity and normal metallic conduction lies in the fact that in the former the current carriers are pairs of electrons (Cooper pairs), while in the latter, to a first approximation, the electrons move independently. Interaction between electrons and lattice vibrations is the most common means of overcoming the Coulomb repulsion, creating a modest attractive poten-

Table 1. Structures and Physical Properties of BEDT-TTF Charge-Transfer Salts Containing Trisoxalatometalate Anions: (BEDT-TTF)$_n$[AM(C$_2$O$_4$)$_3$]·Solvent

A	M	solvent	packing	electrical properties	magnetic properties[a]	ref
NH_4	Fe	C_6H_5CN	layers of pseudo-κ donors anion layers	semiconductor (σ_{RT} = 2×10^{-4} S·cm^{-1}; E_a = 0.140 eV)	PM: C = 4.37 emu·K·mol^{-1}; θ = −0.11 K	16
K	Fe	C_6H_5CN	same as above	semiconductor (σ_{RT} = 10^{-4} S·cm^{-1}; E_a = 0.141 eV)	PM: C = 4.44 emu·K·mol^{-1}; θ = −0.25 K	16
NH_4	Co	C_6H_5CN	same as above	semiconductor (E_a = 0.225 eV)	DM	17a
NH_4	Al	C_6H_5CN	same as above	semiconductor (E_a = 0.222 eV)	DM	17a
H_3O	Cr	C_6H_5CN	same as above	semiconductor (E_a = 0.153 eV)	PM: C = 1.73 emu·K·mol^{-1}; θ = −0.88 K	17a
H_3O	Cr	C_6H_5CN	β'' donor layers anion layers	superconductor (T_c = 6 K; H_c = 100 Oe)	PM: C = 1.96 emu·K·mol^{-1}; θ = −0.27 K	17b
H_3O	Fe	C_6H_5CN	same as above	superconductor (T_c = 8.3 K; H_c = 500 Oe)	PM: C = 4.38 emu·K·mol^{-1}; θ = −0.2 K	16
H_3O	Cr	$C_6H_5NO_2$	same as above	superconductor (T_c = 6 K; H_c = 100 Oe)	PM	25
H_3O	Fe	$C_6H_5NO_2$	same as above	superconductor (T_c = 4 K; H_c = 50 Oe)	PM	25
H_3O	Fe	C_5H_5N	same as above; 1/4 donors disordered	metal−insulator transition at 116 K	PM	18
H_3O	Cr	CH_2Cl_2	same as above; 1/4 donors disordered	metal−insulator transition at 200 K	PM	19

[a] PM = paramagnetic.

tial. However, the presence of a magnetic field can overcome the pairing energy and return the superconductor to the normal state. Thus, superconductors are characterized by critical field as well as critical temperature. However, not only externally applied fields are effective; in a ferromagnet there is the internal field due to the ordered moments, while even in antiferromagnets or paramagnets there are local fields. It has therefore been pointed out with justice that magnetism and superconductivity are inimical to each other. Ginzburg[5] first pointed out that coexistence between superconductivity and ferromagnetism was impossible.

In conventional superconductors, even a few percent of paramagnetic impurity atoms in the lattice are sufficient to suppress superconductivity.[6] The first compounds in which long-range magnetic order and superconductivity both figured were discovered in the 1970s, with the ternary lanthanide Rh borides and Chevrel phases $LnMo_6S_8$.[7,8] On lowering the temperature, the former first become superconducting (e.g. T_{c1} is 8.9 K for the Er compound) but then return to the normal state ($T_{c2} \sim 0.9$ K in $ErRh_4B_4$) when they become ferromagnetic. There is even a narrow temperature range just above T_{c2} over which the two states coexist, although the magnetic order is not collinear ferromagnetic but sinusoidal.[9,10] It is certainly significant that in both series of compounds the source of the magnetic moments is the 4f lattice of lanthanide ions, while the superconductivity comes from conduction bands formed mainly from the 4d orbitals of the transition metal. Any exchange interaction is undoubtedly very weak, because of the large distance between the two kinds of ion and small f−d orbital overlap. Similar considerations are likely to apply in the magnetic molecular charge-transfer salts, where cations and anions are widely separated. One recent example of an oxide superconductor is even more spectacular: $RuSr_2GdCu_2O_8$ has a layer structure reminiscent of the high-temperature cuprate superconductors, with double CuO_4 layers alternating with layers of corner-sharing RuO_6 octahedra interspersed with Gd and Ba. It becomes ferromagnetic at 132 K and superconducting at 40 K, without loss of ferromagnetism.[11] The astonishing lack of impact of the magnetic order on the superconductivity has been ascribed to a fortuitous effect of crystal symmetry, ensuring that nodes in the conduction electron density occur exactly at the magnetic centers.

Several of the $LnMo_6S_8$ phases become antiferromagnetic rather than ferromagnetic at low temperature, and in these cases the superconductivity is not suppressed.[12,13] For example, T_c and T_N are respectively 1.4 and 0.8 K for $GdMo_6S_8$. This is because the localized magnetic moments vanish when averaged over the scale of the superconductivity coherence length of around 100 Å. However, the critical field is influenced by the onset of long-range antiferromagnetic order, being decreased below T_N in $LnMo_6S_8$ (Ln = Gd, Tb, Dy) but enhanced in $SmRh_4B_4$.

What differentiates molecular materials from the extended inorganic solids is that the interactions between the two molecular networks can be made very weak, since the intermolecular contacts are of the van der Waals type or hydrogen bonds. The usual combination of a discrete magnetic anion with an oxidized organic donor may be appropriate to obtain a material exhibiting conductivity or even superconductivity, but most probably the magnetic network will behave as a paramagnet down to very low temperatures. This is the case of the two series of magnetic superconductors so far discovered which are based on the mononuclear metal complexes trisoxalatometalate $[M(C_2O_4)_3]^{3-}$ (M^{III} = Fe, Cr) and tetrahalometalate $[MX_4]^-$ (X = Cl, Br; M^{III} = Fe) (sections 2.1 and 2.2 and Tables 1 and 2). A rational strategy to introduce ferromagnetism in the material

Table 2. Structures and Physical Properties of Charge-Transfer Salts Containing Tetra- and Hexahalogenometalate Anions

compound	packing	electrical properties	magnetic properties[a]	ref
(TMTTF)[$FeCl_4$]	orthogonal linear stacks; isolated anions	insulator (σ_{RT} > 10^{-5} S·cm^{-1})	PM; $\theta = -5$ K	44
(TMTSF)[$FeCl_4$]	two independent linear stacks; isolated anions		AFM below 4 K; $C = 4.2$ emu·K·mol^{-1}; $\theta = -7.5$ K	46
(perylene)$_3$[$FeCl_4$]	stacks of donor tetramers; anions in pairs	semiconductor ($\sigma_{RT} = 0.17$ S·cm^{-1}; $E_a = 0.12$ eV)	dimers of $FeCl_4^-$; $J = -1.26$ K	54
(perylene)$_3$[$FeBr_4$]	stacks of donor tetramers; anions in pairs	semiconductor	dimers of $FeBr_4^-$; $J = -3.72$ K	54
(TTF)$_{14}$[$MnCl_4$]$_4$	TTF trimers and monomers; isolated anions	semiconductor ($\sigma_{RT} = 0.15$ S·cm^{-1}; $E_a = 0.2$ eV)	PM; $C = 1.14$ emu·K·mol^{-1}; $\theta = -4$ K	55, 56
(TTF)$_{14}$[$CoCl_4$]$_4$	same as Mn salt	semiconductor ($\sigma_{RT} = 0.15$ S·cm^{-1}; $E_a = 0.2$ eV)	PM; $C = 0.657$ emu·K·mol^{-1}; $\theta = -4$ K	55, 56
(TTF)[$MnCl_3$]$_{\sim 0.75}$	no structure	semiconductor ($\sigma_{RT} = 15$ S·cm^{-1}; $E_a = 0.1$ eV)	AFM Mn^{2+} chain; $C = 3.50$ emu·K·mol-^{1}; $\theta = -14$ K	55
(BEDT-TTF)[$MnCl_4$]$_{0.3-0.4}$	no structure	semiconductor ($\sigma_{RT} = 0.5$ S·cm^{-1})	PM; $C = 1.30$ emu·K·mol^{-1}; $\theta = -1$ K	57
(BEDT-TTF)[$CoCl_4$]$_{0.3-0.4}$	no structure	semiconductor ($\sigma_{RT} = 0.5$ S·cm^{-1})	PM; $C = 0.87$ emu·K·mol^{-1}; $\theta = -1.3$ K	57
(BEDT-TTF)$_3$[$MnCl_4$]$_2$	β' donor layers; $MnCl_4$ layers	semiconductor ($\sigma_{RT} = 25$ S·cm^{-1}; $E_a = 0.04$ eV)		58
(BEDT-TTF)$_3$[$CuBr_4$]	α-stacked layers; planar $CuBr_4^{2-}$	semiconductor ($\sigma_{RT} = 0.25$ S·cm^{-1}; $E_a = 0.07$ eV)	AFM; $C = 2.77$ emu·K·mol^{-1}; $\theta = -140$ K; 1st order transition 59 K	68, 74
(TTMTTF)[$CuBr_4$]	nonplanar $TTMTTF^{2+}$	insulator ($\sigma_{RT} = 10^{-10}$ S·cm^{-1})	PM; $\theta = -0.5$ K	74
(BETS)$_2$[$FeCl_4$]	λ donor stacks; anion layers	metal−insulator transition 8.5 K; superconducting > 3.2 kbar	AFM; TN = 8.5 K	27
(BETS)$_2$[$FeCl_4$]	κ donor stacks; anion layers	superconducting: $T_c = 0.1$ K	AFM; TN = 0.45 K	39
(BETS)$_2$[$FeBr_4$]	κ donor stacks; anion layers	superconducting: $T_c = 1.1$ K	AFM; TN = 2.5 K	38
(BET-TTF)$_2$[$FeCl_4$]	2 types of donor layers; isolated anions	metal−insulator transition ~20 K	PM; Fe···Fe AFM dimers at low temperature ($J = -0.22$ K)	61
(BEDT-TTF)$_2$[$FeCl_4$]	layers of dimerized stacks; layers of anions	semiconductor: $E_a = 0.21$ eV	PM; $\theta = -4$ K	47
(BEDT-TTF)[$FeBr_4$]	donors dimerized; no stacks	insulator	PM	47
(BEDT-TTF)$_3$[$CuCl_4$]·H_2O	layers of stacked trimerized donors; layers of anions	metal	PM	62
(BEDT-TTF)$_3$[$NiCl_4$]·H_2O	layers of stacked trimerized donors; layers of anions	metal−insulator transition 100 K		73
(BEDT-TTF)$_2$[$ReCl_6$]·C_6H_5CN	layers of π-stacked donors; layers of $ReCl_6$ and C_6H_5CN	semiconductor ($\sigma_{RT} = 3$ S·cm^{-1}; $E_a \sim 0.07-0.15$ eV)	PM; $C = 1.10$ emu·K·mol^{-1}; $\theta = -0.14$ K	76
(BEDT-TTF)$_2$[$IrCl_6$]	3D lattice of donor dimers and anions	semiconductor ($\sigma_{RT} = 10^{-2}$ S·cm^{-1}; $E_a = 0.23$ eV)	PM; $C = 0.234$ emu·K·mol^{-1}; $\theta = -0.37$ K	76

[a] PM = paramagnetic; AFM = antiferromagnetic.

is to use as inorganic anion an extended magnetic layer, such as, for example, the bimetallic oxalato complexes. However, this novel approach requires the formation of the layered network at the same time that the organic donor is oxidized. As we can imagine, the crystallization of such a hybrid is not an easy task. Furthermore, even if one succeeds in getting crystals from such a combination, that does not guarantee the superconductivity in the organic network, as no control on the packing and oxidation state of the donor is possible. Thus, the design and crystallization of a ferromagnetic molecular superconductor remains a chemical challenge.

2.1. BEDT-TTF Salts with Trisoxalatometalate(III) Anions

Over the past few years numerous examples have been found of two-dimensional bimetallic layers containing dipositive cations, M^{II}, and trisoxalatometalate(III) anions, in which the oxalate ion acts as bridging ligand, forming infinite sheets of approximately hexagonal symmetry, separated by bulky organic cations.[14,15] In view of the unusual magnetic properties of these compounds, the synthesis of compounds containing similar anion lattices but interleaved with BEDT-TTF molecules has been explored.

A number of such compounds have been characterized to date and prove to have a rich variety of structures and properties, among them being superconductivity. The first series is $(BEDT\text{-}TTF)_4[AM(C_2O_4)_3]\cdot$solvent (Table 1) ($A^+ = H_3O$, K, NH_4; M(III) = Cr, Fe, Co, Al, Ga; solvent = C_6H_5CN, $C_6H_5NO_2$, C_5H_5N).[16−19] While the stoichiometry is the same in all the compounds, the structures fall into two distinct series with contrasting physical properties. One, which is orthorhombic (*Pbcn*), is semiconducting, with the organic molecules present as $(BEDT\text{-}TTF)_2^{2+}$ and $(BEDT\text{-}TTF)^0$, while the other, which is monoclinic (*C*2/*c*), has BEDT-TTF packed in the β'' arrangement[16] and is the first example of a molecular superconductor containing a lattice of paramagnetic ions.[20]

The crystal structures of both series of compounds consist of alternate layers containing either BEDT-TTF or $[AM(C_2O_4)_3]\cdot$solvent. The anion layers contain alternating A and M forming an approximately hexagonal network (Figure 2). The M are octahedrally coordinated by three bidentate oxalate ions, while the O atoms of the oxalate which are not coordinated to M form cavities occupied by A. The solvent molecules occupy roughly hexagonal cavities in the $[AM(C_2O_4)_3]$ lattice. Chirality is a further unusual feature of the anion layers. The point symmetry of $[M(C_2O_4)_3]^{3-}$ is D_3, and the ion may exist in two enantiomers. In the monoclinic superconductors alternate anion layers are composed exclusively either of one or the other, while in the orthorhombic semiconductors the enantiomers are arranged in alternate columns within each layer.

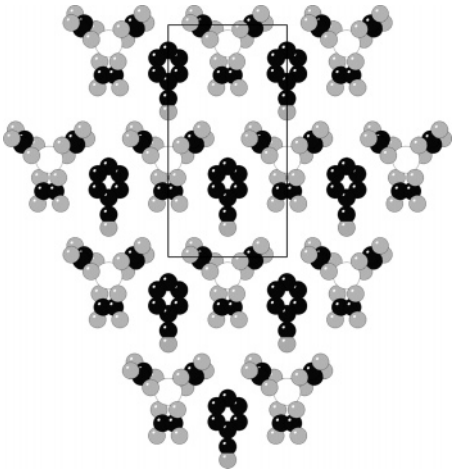

Figure 2. Schematic view of the anion layer in $(BEDT\text{-}TTF)_4[AM(C_2O_4)_3]\cdot$solvent (solvent = C_6H_5CN).

Although the anion layers are very similar, the molecular arrangements in the BEDT-TTF layers are quite different in the orthorhombic and monoclinic series. In the monoclinic phases there are two independent BEDT-TTF, whose central C=C bond lengths differ markedly, indicating charges of 0 and +1. The +1 ions occur as face-to-face dimers, surrounded by monomeric neutral molecules (Figure 3). Molecular planes of neighboring dimers along [011] are oriented nearly orthogonal to one another, as in the κ-phase structure of $(BEDT\text{-}TTF)_2X$,[21] but the planes of the dimers along [100] are parallel. This combination of

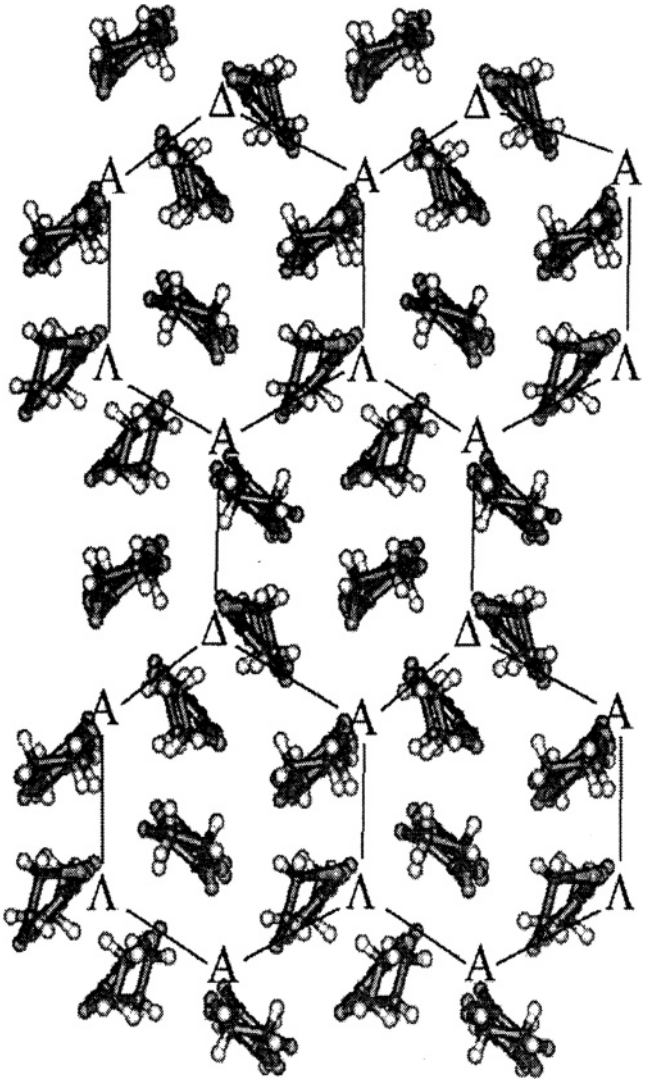

Figure 3. Packing of the BEDT-TTF in the orthorhombic series $(BEDT\text{-}TTF)_4[AM(C_2O_4)_3]\cdot$solvent. (Reprinted with permission from ref 17a. Copyright 2001 American Chemical Society.)

$(BEDT\text{-}TTF)_2^{2+}$ surrounded by $(BEDT\text{-}TTF)^0$ has also been observed[22] in a BEDT-TTF salt with the polyoxometalate $\beta\text{-}[Mo_8O_{26}]^{4-}$. The $(BEDT\text{-}TTF)^0$ describe an approximately hexagonal network, while the $(BEDT\text{-}TTF)_2^{2+}$ are positioned near the oxalate ions, with weak H-bonding between the terminal ethylene groups and oxalate O. Packing of the BEDT-TTF in the *C*2/*c* salts is quite different: there are no discrete dimers but stacks with short S···S distances between them, closely resembling the β''-structure in metallic $(BEDT\text{-}TTF)_2AuBr_2$[23] and the pressure-induced superconductor $(BEDT\text{-}TTF)_3Cl_2\cdot 2H_2O$[24] (Figure 4).

While the orthorhombic salts are semiconductors, the monoclinic ones are metals with conductivity of $\sim 10^2$ S·cm^{-1} at 200 K, decreasing monotonically by a factor of about 8 down to temperatures between 7 and 8 K[16] (A = H_3O^+; M = Fe; solvent = C_6H_5CN) and down to 3 K[24] ($A^+ = H_3O^+$; M = Cr; solvent = $C_6H_5NO_2$), where they become superconducting (Figure 5, top).

In line with their contrasting electrical behavior, the magnetic properties of the two series are also quite different. The susceptibilities of the semicon-

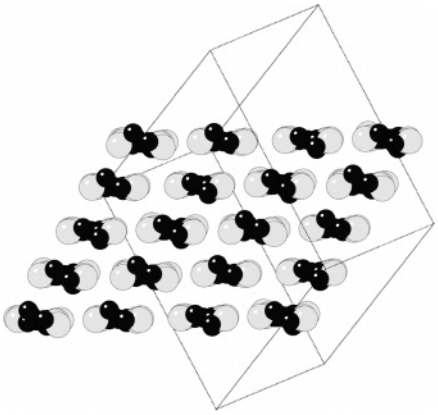

Figure 4. Packing of the organic layers in the monoclinic series (BEDT-TTF)$_4$[AM(C$_2$O$_4$)$_3$]·solvent showing the β''-structure.

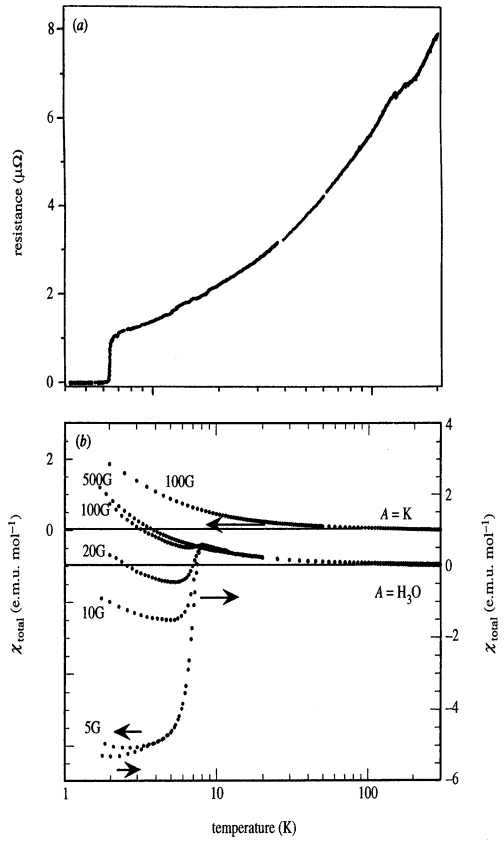

Figure 5. Temperature dependence of the resistivity (top) and the magnetic susceptibility (bottom) of β''-(BEDT-TTF)$_4$[(H$_3$O)Fe(C$_2$O$_4$)$_3$]·C$_6$H$_5$CN. On the bottom the susceptibility of (BEDT-TTF)$_4$[KFe(C$_2$O$_4$)$_3$]C$_6$H$_5$CN is also shown. (Reprinted with permission from ref 16. Copyright 1995 American Chemical Society.)

ducting compounds obey the Curie−Weiss law from 2 to 300 K with the M dominating the measured moment. In particular, there is little contribution from the BEDT-TTF, including those molecules whose bond lengths suggest a charge of +1. Hence, the (BEDT-TTF)$_2^{2+}$ are spin-paired in the temperature range studied (the singlet−triplet energy gap is expected to be >500 K), while the remaining BEDT-TTF do not contribute to the paramagnetic susceptibility, in agreement with the assignment of zero charge. On the other hand, the superconducting salts obey the Curie−Weiss law from 300 to about 1 K above T_c, though with a temperature independent paramagnetic contribution. The measured Curie constants are close to that predicted for M^{3+} (Cr, Fe), while the Weiss constants (−0.2 K) signify very weak antiferromagnetic exchange between the M(III) moments. However, there is a strong diamagnetic contribution in the superconducting temperature range, returning to Curie−Weiss behavior above 10 K (Figure 5, bottom). While the EPR spectrum of the semiconducting A = K, M = Fe compound consists of a single narrow resonance, that of the A = H$_3$O, M = Fe compound consists of two resonances: a narrow one assigned to the Fe(III) by analogy with the A = K compound, and a much broader resonance from the conduction electrons. This situation is reminiscent of that found in (BEDT-TTF)$_3$[CuCl$_4$]·H$_2$O (see section 3.1.1).

Recently, high frequency (71.3 GHz) EPR measurements on the A = H$_3$O, M = Fe superconductor, with the applied field perpendicular to the conducting planes, have revealed the five-line spectrum anticipated for the $S = {}^5/_2$ Fe^{3+}. The spectrum is unchanged on passage from the normal to superconducting state but undergoes a monotonic shift from 20 to 1.4 K, with an incipient splitting at the lowest temperature, which may signify the onset of short-range magnetic correlations in the anion layer.[26]

2.2. BETS Salts with Halometalate Anions

Among the large variety of conducting charge-transfer salts containing monomeric transition metal anions, very few show clear experimental evidence of interaction between the pπ and d electron sublattices. In particular, changes in conduction that can be associated with ordering of d moments are quite difficult to identify. Consequently, there has been a lot of interest in the contrasting behavior in two isomorphous salts λ-(BETS)$_2$MCl$_4$ depending on whether M is the closed-shell Ga^{III} or $S = {}^5/_2$ Fe^{III} (Figure 6). A detailed account of the properties of these fascinating materials is given in this volume by Kobayashi, but for completeness we summarize the salient facts here (see Table 2). Both are metals, but whereas the former becomes superconducting at 8.5 K, the latter undergoes antiferromagnetic order accompanied by a sharp metal−insulator transition almost at the same temperature.[27] A clear correlation between magnetic ordering and the conduction is identified by the observation that the metallic state can be re-established at low temperature on applying fields in excess of 11 T, under which conditions the Fe moments became saturated ferromagnetically.[28,29]

On the other hand, more recent studies of the variation of the conductivity of both salts with pressure throw some doubt on the significance of the magnetic transition in bringing about the metal−insulator transition. In fact, the metal−insulator transition temperature falls with increasing hydrostatic pressure until it transforms sharply into a transition to a superconducting state at 3.2 kbar. The latter transition takes place at 1.8 K and decreases with increasing pressure, as in most molecular superconductors. At the same pressure, T_c of the Ga salt is 3.0 K, with nearly identical pressure depen-

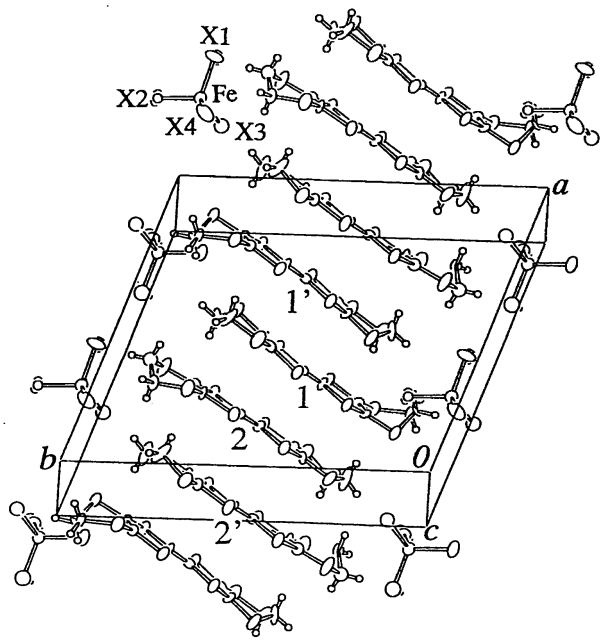

Figure 6. Crystal structure of λ-(BETS)$_2$[FeX$_4$] (X = Cl, Br). (Reprinted with permission from ref 27. Copyright 1996 American Chemical Society.)

dence,[30] suggesting that the properties of the conduction electrons are very similar in the nonmagnetic and magnetic salts. The phase diagram of the $[FeCl_4]^-$ salt is shown in Figure 7 (top) in the P,T-plane. This

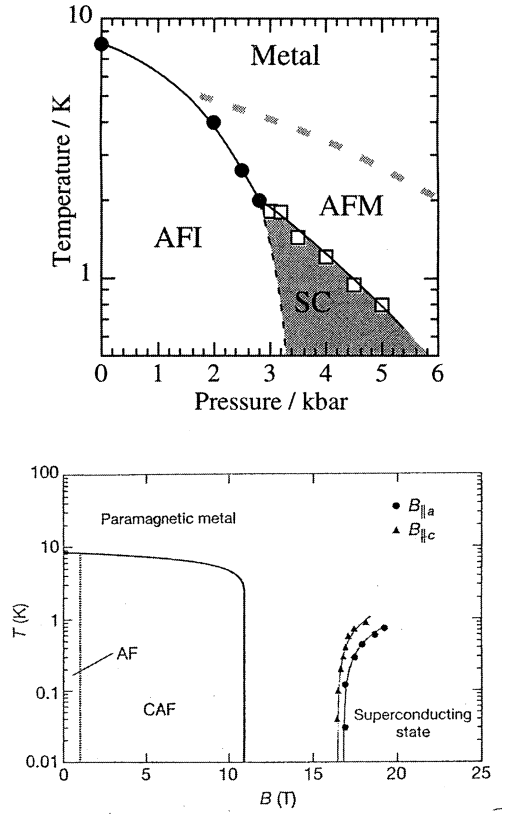

Figure 7. Electronic phase diagram of λ-(BETS)$_2$[FeCl$_4$] in (top) the P,T-plane[32] and (bottom) the H,T-plane. (Reprinted with permission from *Nature* (http://www.nature.com), ref 32. Copyright 2001 Nature Publishing Group.)

different low temperature conduction at ambient pressure is therefore most likely to be due to the small difference in their unit cell volumes.

Above 3.5 kbar λ-(BETS)$_2$FeCl$_4$ is an antiferromagnetic metal above T_c, with a peak in the susceptibility at 4 K and typical spin flip behavior at high field.[31] However, it was reported that in fields above 17 T this salt becomes superconducting,[32] and Figure 7 (bottom) shows the phase diagram in the H,T-plane. It has since been shown that this field-stabilized superconducting state reverts to the normal metallic state above 42 T.[33] Furthermore, in crystals where the Fe is diluted with Ga, the superconducting phase remains stable in lower magnetic fields as the Ga concentration is increased[34−36] (Figure 8). To explain

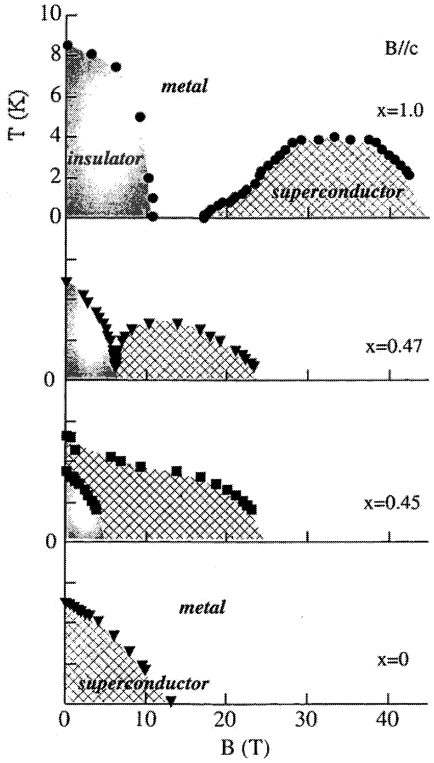

Figure 8. Superconducting properties of solid solutions of Fe/Ga in the λ-(BETS)$_2$[MCl$_4$] phase (M = Fe, Ga). (Reprinted with permission from ref 34. Copyright 2003 Elsevier.)

this unusual field dependent behavior, it has been suggested that the applied magnetic field serves to cancel the $\pi-d$ exchange field in the conducting layers. This so-called Jaccarino−Peter effect was first observed in the Chevrel phase magnetic superconductors.[37] The effects of tilting the applied field have also been comprehensively studied, as has the effect of pressure on the transition.[34]

In the BEDT-TTF salts, many superconductors have the κ-phase stacking arrangement, in which face-to-face dimers are organized with the planes of near neighbors orthogonal. It is therefore of great interest to observe the properties of κ-phase BETS salts, bearing in mind that the latter have more stable metallic states because of replacement of S by Se in the central part of the molecule. Both $[FeCl_4]^-$ and $[FeBr_4]^-$ salts with this structure have been reported; both are antiferromagnetic superconductors,[38,39] with T_N and T_c being much lower in the chloride than the bromide. In the chloride salt, the resistivity changes at T_N, which could be taken as

evidence in this case that the π and d electrons interact. On the other hand, it may be the result of a small movement in the lattice, possibly as a result of magnetostriction. Further, while the magnetic phase transition in the $[FeBr_4]^-$ salt is fully three-dimensional, the temperature dependence of the heat capacity in the $[FeCl_4]^-$ case reveals considerable two-dimensional character, since the magnetic entropy only reaches 86% of its saturation value as high as $3T_N$. Most likely, the more polarizable Br furnishes a more effective exchange pathway than Cl.

In contrast to λ-$(BETS)_2FeCl_4$, where there are numerous close halogen−chalcogen contacts that facilitate π−d interaction, in κ-$(BETS)_2FeBr_4$ no such close contacts are found. Consequently, the metallic state remains unaffected, where the Fe^{3+} moments order antiferromagnetically, with the antiferromagnetic superconducting state being established at lower temperature. Furthermore, the $FeBr_4$ salt behaves as a metamagnet, undergoing an abrupt transition from antiferromagnetic to a saturated paramagnetic (forced ferromagnetic) state at 1.6 T.[38] Significantly, this is precisely the field at which the superconducting state reverts equally sharply to metallic,[39] so it is a plausible hypothesis that the internal field generated by the field-induced ferromagnetic saturation of the Fe^{3+} moments destroys the superconductivity. Because the transition is so abrupt, it is even possible to modulate the resistance by periodically modulating the applied field.[40]

3. Magnetic Metals and Semiconductors

The combination of magnetic moments with conduction electrons in the same molecular material may give rise to a simple superposition of magnetic and conducting properties when the two sublattices are electronically independent, or to a mutual influence between these properties when they interact. In this latter case the interaction between the two networks may induce exchange coupling between the localized magnetic moments through a mechanism that resembles the so-called RKKY-type of exchange proposed in the solid state to explain the magnetic interactions in transition and rare-earth metals and alloys.[4] This kind of indirect interaction is long-range, in contrast to the superexchange one, and presents an oscillatory behavior, which can give rise alternately to ferro- or antiferromagnetic coupling, depending on the distance between the moments. In the lanthanide metals for example, the partly filled 4f shells, which do not overlap significantly with neighboring orbitals, give rise to strongly localized magnetic moments. Therefore, the coupling between these f electron moments occurs via the conduction electrons (mainly of s-type) which are strongly coupled with the f electrons. Thanks to this intra-atomic f−s coupling, the f electrons at a given site strongly polarize the spins of those conduction electrons in the vicinity. This local polarization leads to a modulation of the electron densities in the band which is different for the up and down spins. A second magnetic ion, situated at a certain distance from this ion, will be informed by the conduction electrons of its spin direction. As a result, these two localized magnetic moments will be coupled by an effective coupling J_{ind}. The sign and magnitude of this indirect coupling are given by the following expression:

$$J_{ind} = \frac{9\pi}{2}\frac{J_{dir}^2}{E_F}\left(\frac{n}{N}\right)^2 F(2k_F R)$$

where J_{dir} is the direct interaction between localized and itinerant spins, n/N is the number of conduction electrons per magnetic site, and $(2m_e E_F/\hbar)^{1/2}$ is the momentum of the electron at the Fermi level, E_F.

Therefore, this indirect interaction is expected to be proportional to the direct interaction between localized and itinerant spins. Its strength decreases as $1/R^3$, where R is the distance between the magnetic sites, in the same way as a dipolar interaction. Its sign is determined by the oscillating function $F(x)$, which can give either ferromagnetic or antiferromagnetic coupling between the magnetic sites depending on their separation R (Figure 9). The period for these

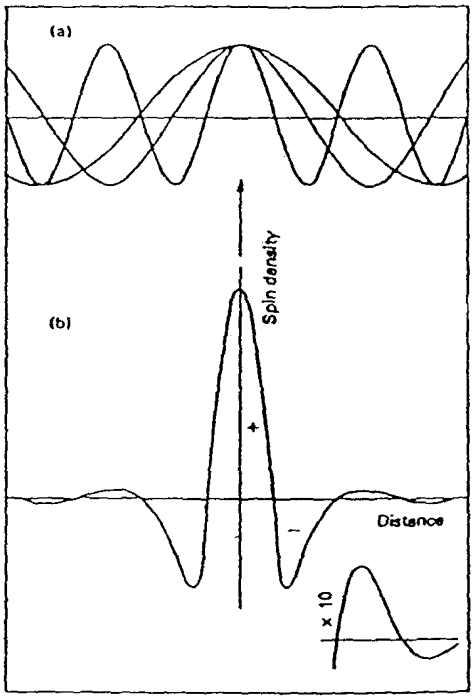

Figure 9. Oscillating exchange interaction with distance between two localized moments in the RKKY model.

oscillations depends on the concentration of conduction electrons, n, since in the free electron model $k_F = (3/8\pi n)^{1/3}$.

In molecular conductors containing discrete magnetic anions, an indirect exchange interaction between the magnetic moments via the conduction electrons is, in principle, possible. However, its strength is expected to be quite small, as the direct interaction between the two networks via a coupling between the itinerant π electrons and the d electrons of the magnetic center is also very weak. Still, the physics associated with this exchange interaction may differ in several respects from the one predicted by the RKKY model. Thus, the model assumes that the conduction electrons can be described by the free electron model. In molecular conductors this model

is too crude, as the electrons are strongly correlated; furthermore, the molecular systems have low dimensional electronic structures. Furthermore, in classical metals the direct interaction involves an intra-atomic coupling between the unpaired electrons of the metal (d or f) and the s electron carriers, while in the magnetic synthetic metals this interaction involves an intermolecular $\pi-$d coupling. These important differences justify the effort currently being devoted to preparing and physically characterizing this novel type of molecular material.

It is worth mentioning that the association between cation-radicals and magnetic anions is not the only way to obtain molecular materials having conducting electrons and localized magnetic moments. Materials formed by a single network can also provide examples of this kind. An illustrative example is the compound $[Cu(pc)]^{0.33+}[I_3^-]_{0.33}$ (pc = phthalocyanine).[41,42] The compound is a one-dimensional metal formed by columnar stacks of partially oxidized Cu(pc) units separated by a distance of 3.2 Å. The electron delocalization occurs through the overlap between the π-molecular orbitals of aromatic rings of adjacent phthalocyanine molecules. The paramagnetic Cu(II) ions are embedded in this "Fermi sea" of itinerant electrons. Owing to the large Cu−Cu distance, the Cu^{2+} ions are expected to be magnetically uncoupled. However, coupling between the Cu^{2+} local moments (represented as J_{d-d} in Figure 10) of ~6 K has been

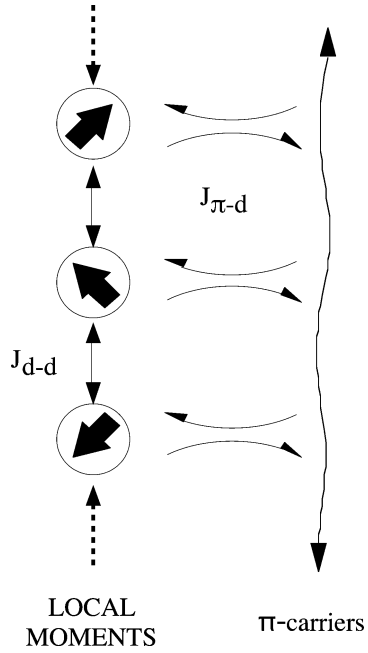

Figure 10. Coupling between Cu^{2+} moments in $[Cu(Pc)]^{+0.33}(I_3^-)^{-0.33}$.

detected by EPR, NMR, and magnetic susceptibility studies. It has been proposed that such coupling occurs through the conduction electrons which are strongly coupled to the local magnetic moments ($J_{\pi-d}$ coupling).

3.1. Mononuclear Metal Complexes

3.1.1. Tetrahalometalates

Following the discovery of the first molecular charge-transfer salts that behaved as superconductors, many attempts have been made to synthesize analogous compounds containing paramagnetic moments inside the lattice. The so-called Bechgaard salts[43] of TTF, TMTTF, and TMTSF contain diamagnetic tetrahedral and octahedral anions such as $[ClO_4]^-$ and $[PF_6]^-$, so it was natural to seek examples with tetra- and hexahalometalates. These examples are summarized in Table 2. The first such compound whose structure was determined, (TMTTF)$[FeCl_4]$, however, has not only a different stoichiometry from the 2:1 Bechgaard salts but a completely different packing of the donor molecules, which form stacks but with alternate long axes orthogonal and no significant interaction between them, although there are several S···Cl contacts of less than the sum of the van der Waals radii.[44] Both this salt and one containing $[MnCl_4]^{2-}$ are semiconductors and paramagnets with small negative Weiss constants. The corresponding Se salt (TMTSF)$[FeCl_4]$ was shown to contain two kinds of columnar stacks, one with the long molecular axes parallel and the other with it orthogonal, as in the TMTTF salt.[45] Curiously, this structure was reported again, quite independently and without reference to the earlier work.[46] The magnetic properties are dominated by the Fe, with χT at room temperature reaching 4.2 emu·K·mol^{-1} (cf. 4.375 for $S = 5/2$). The $[FeCl_4]^-$ are well isolated, though as in the TMTTF salt, there are Se···Cl close contacts. There is a small negative Weiss constant (−7.5 K), but significantly, the susceptibility becomes anisotropic below 4 K, suggesting the onset of antiferromagnetism.[46]

The tetrahaloferrate(III) salts of the extended electron donor BEDT-TTF present a fascinating contrast.[47] Electrochemical synthesis under the same conditions yielded different chemical stoichiometries for the salts containing $[FeCl_4]^-$ and $[FeBr_4]^-$. The structure of (BEDT-TTF)$_2[FeCl_4]$ consists of dimerized stacks of BEDT-TTF molecules separated by the sheets of tetrahedral $[FeCl_4]^-$ anions. The anions are situated in an "anion cavity" formed by the ethylene groups of the BEDT-TTF molecules, which are arranged in the sequence ...XYYXXYYX... (Figure 11). Adjacent molecules of the same type (XX′ and YY′)

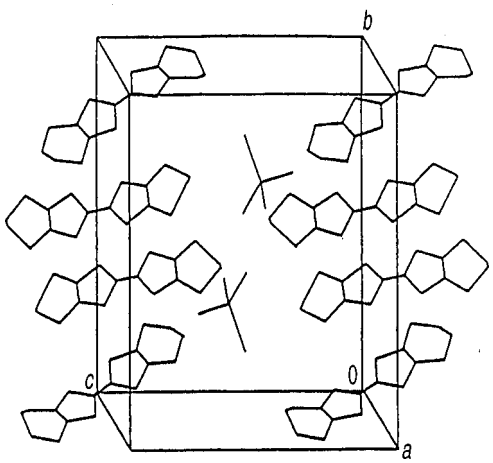

Figure 11. Crystal structure of (BEDT-TTF)$_2[FeCl_4]$, showing the XXYYXX stacking sequence of donor cations. (Reprinted with permission from ref 47. Copyright 1990 Royal Society of Chemistry.)

stack uniformly on top of each other but with a slight displacement between neighbors along the long in-plane molecular axis. On the other hand, the long in-plane molecular axes of adjacent molecules of different type (XY′ and YX′) are rotated relative to one another. Furthermore, X and X′ (or Y and Y′) are closer to each other (≈3.60 Å) than X and Y (3.81 Å). The shortest distances between BEDT-TTF molecules are shorter than the sum of the van der Waals radii of two sulfur atoms (3.60 Å), thus suggesting the possibility of a quasi-one-dimensional interaction along the *a* direction.

On the other hand, in (BEDT-TTF)[$FeBr_4$], there are no stacks but planes of closely spaced BEDT-TTF, in marked contrast to most of the compounds containing this donor molecule. The only short S···S distances (<3.50 Å) are between two BEDT-TTF molecules in different pairs, but there is no continuous network of short S···S contacts through the lattice. The $[FeBr_4]^-$ form a three-dimensional lattice separated by the pairs of BEDT-TTF molecules. One $[FeBr_4]^-$ has short intermolecular distances to two donor molecules, but no extended interaction between BEDT-TTF molecules through the $[FeBr_4]^-$ is possible, which correlates with the insulating behavior of this compound.

The structure of the $FeCl_4^-$ salt is closely related to those of (BEDT-TTF)$_2$[$InBr_4$],[48] α-(BEDT-TTF)$_2$[PF_6],[49] *β*-(BEDT-TTF)$_2$[PF_6],[50] and (BEDT-TTF)$_2$[AsF_6],[51] with the salts containing octahedral anions exhibiting interstack side-by-side contact distances nearly identical to those found in (BEDT-TTF)$_2$[$FeCl_4$]. There are no short contact distances between sulfur atoms along the molecular stacking direction in any of these compounds, and so their conduction properties are highly one-dimensional. For example, in *β*-(BEDT-TTF)$_2$[PF_6] the ratio of the conductivities along the direction of side-by-side contacts to those along the molecular stacking direction is 200:1.[49,50] (BEDT-TTF)$_2$[$FeCl_4$] is also semiconducting, like the PF_6 and AsF_6 salts, with an activation energy of 0.21 eV.

Given that the formal charge per donor molecule is $+^1/_2$ in the $[FeCl_4]^-$ salt, the unpaired spins on the organic cations contribute to the susceptibility. For example, the molar susceptibility of (BEDT-TTF)$_2$[$GaCl_4$], which has a similar structure but a diamagnetic anion, has a broad maximum near 90 K, which can be fitted from 70 to 300 K either by a one-dimensional (Bonner−Fisher) or quadratic layer antiferromagnetic model to yield exchange parameters J/k of respectively 66.5(5) and 89.6(1) K, similar to those found in the semiconducting α′-(BEDT-TTF)$_2$X with X = $AuBr_2$, $Ag(CN)_2$, or $CuCl_2$,[52] where the absolute values of the susceptibility agree with expectations for localized moments corresponding to $S = ^1/_2$ per pair of donor molecules. In the $[FeCl_4]^-$ salt, on the other hand, the susceptibility is dominated by the anion. From the low-temperature data, a value of the Weiss constant can be extracted and the parameters of the fit ($S = ^5/_2$, $g = 2$, $\theta = -4$ K) can be used to calculate the difference between observed and calculated susceptibility at all temperatures to obtain the contribution from the BEDT-TTF. The resulting difference gives a good fit to a singlet−triplet model (Figure 12).[53]

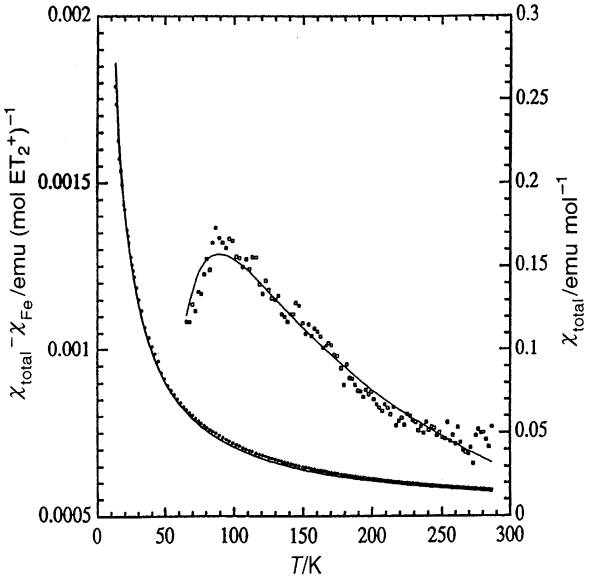

Figure 12. Total susceptibility of (BEDT-TTF)$_2$[$FeCl_4$] (circles) and the BEDT-TTF contribution (squares). (Reprinted with permission from ref 53. Copyright 1996 American Chemical Society.)

Apart from the organo-chalcogen donors, conducting charge-transfer salts are known with various condensed ring aromatic molecules, of which the most extensively studied is perylene (Per) (Chart 1). Thus, it was pertinent to make salts of this donor with transition metal-containing anions. The crystal structures of compounds with the stoichiometry (Per)$_3$[FeX_4] (X = Cl, Br) consist of stacks of tetramerized Per_4 and $[FeX_4]^-$.[54] The $[FeX_4]^-$ are located in pairs, but with quite a large separation between the Fe (∼7.9 Å). The Cl compound is a semiconductor with a high room temperature conductivity (0.175 S·cm^{-1}) and an activation energy of 0.12 eV. Magnetically, the properties are dominated by the Fe, and no long range order is reported, though the reported Weiss constants ($FeCl_4$, −12.1 K; $FeBr_4$, −39.9 K) are quite high. On the other hand, the susceptibility at low temperature was fitted to a dimer model with J/k = −1.26 K ($FeCl_4$) and −3.72 K ($FeBr_4$), despite the long distance between the Fe.

Turning to other tetrahalometalate anions, the first reports of TTF salts with Mn and Co tetrahalo anions did not identify either their precise stoichiometry or crystal structure,[55] but later work from the same group[56] defined the unusual composition (TTF)$_{14}$[MCl_4]$_4$ for M = Mn, Co, Zn, and Cd. The donor molecules in the monoclinic structure are of two types: each unit cell contains two $(TTF)_3^{2+}$ and a TTF^0 orthogonal to one another, with the anions isolated between the trimers. All three compounds, whether magnetic or not, are semiconducting with high room temperature conductivities in the region of 0.1 S·cm^{-1}. The magnetic behavior of the Mn and Co compounds is simple Curie−Weiss in type, with small negative Weiss constants that may be related to zero-field splitting rather than magnetic exchange.

The stoichiometries of the corresponding BEDT-TTF salts were first deduced by elementary analysis

alone as (BEDT-TTF)$[MCl_4]_{0.3-0.4}$ for M = Mn, Co, Zn,[57] but a crystal structure determination for one example indicates that it is (BEDT-TTF)$_3[MnCl_4]_2$.[58] In the latter structure, there are alternating layers containing, on one hand, BEDT-TTF$^+$ in the β' stacking mode and, on the other, $MnCl_4^{2-}$ together with isolated BEDT-TTF^{2+}. This unusual alternative has also been found in the nonmagnetic salt (BEDT-TTF)$_5[Hg_9Br_{11}]$.[59] Both the structurally characterized salt and the earlier ones are reported as semiconducting with relatively high room temperature conductivities, with (BEDT-TTF)$_3[MnCl_4]_2$, in particular, being much more conducting than is usual for β'-salts. Again, the magnetic behavior appears to be that of a Curie−Weiss paramagnet. In fact, the EPR of a BEDT-TTF−$CoCl_4$ salt (of unspecified formula) is said to contain signals from both conduction electrons and localized 3d moments at low temperature,[60] with the resonance field ΔH of the conduction electrons showing a shift below 100 K. A plot of ΔH^{-1} versus temperature is linear, suggesting that an internal field is produced by the localized 3d moments, whose static susceptibility follows the Curie−Weiss law. In contrast, (TTF)$_2[MnCl_4]$ shows no EPR signal due to TTF$^+$. Observation of two EPR signals in the $CoCl_4$ salt indicates that the two spin systems are behaving essentially independently of each other, as in the BEDT-TTF−$CuCl_4$ salt described below but in contrast to (BEDT-TTF)$_3[CuBr_4]$.

Another interesting example is the radical salt prepared with the BET-TTF donor (Chart 1) and the paramagnetic $[FeCl_4]^-$ anion: β-(BEDT-TTF)$_2[FeCl_4]$.[61] This salt shows a metallic behavior with a room temperature conductivity of 60 S·cm^{-1} and a M−I transition around 20 K. The EPR spectrum of this salt shows a single signal centered at $g = 2.017$ with a line width of 400 G. No signal from the BET-TTF is detected, in contrast with the isostructural salt of the diamagnetic $[GaCl_4]^-$ anion that exhibits a signal at $g = 2.0065$ with a line width of 13 G. Such a feature has been attributed to the presence of a weak exchange interaction between Fe(III) spins through the conducting electrons.

The anions $[CuX_4]^{2-}$ (X = Cl, Br) adopt a wide variety of geometries, from square-planar to flattened tetrahedral, and the crystal structures (and hence properties) of the BEDT-TTF salts with these anions are much more varied and interesting than those of the other 3d ions. Among them is the first example of a metallic molecular charge-transfer salt, (BEDT-TTF)$_3[CuCl_4]\cdot H_2O$,[62] in which magnetic resonance has been observed simultaneously from conduction and localized electrons. Other examples, containing $[CuBr_4]^{2-}$ and $[CuCl_2Br_2]^{2-}$, have the largest change of conductivity with pressure ever seen in conducting organic solids and more substantial interaction between the conduction electrons and 3d moments.

The crystal structure of (BEDT-TTF)$_3[CuCl_4]\cdot H_2O$ consists of stacks of BEDT-TTF parallel to the *c*-axis, with short interstack S−S contacts leading to the formation of layers (Figure 13).[62] The latter are interleaved by the $[CuCl_4]^{2-}$ and H_2O in the same general arrangement as in (BEDT-TTF)$_2FeCl_4$. However, in (BEDT-TTF)$_3CuCl_4\cdot H_2O$ there are three

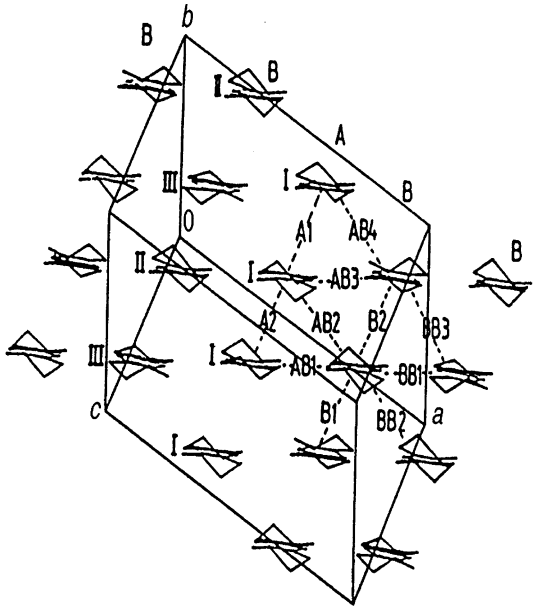

Figure 13. BEDT-TTF layers in (BEDT-TTF)$_3[CuCl_4]\cdot H_2O$. (Reprinted with permission from ref 62a. Copyright 1992 American Chemical Society.)

crystallographically independent BEDT-TTF molecules (I, II, III) and two different stacks (A and B). Stack A contains only BEDT-TTF of type I, and stack B has an alternate arrangement of II and III. Within the *ac*-plane, the stacks form an XYYXYYX array. The anions lie in planes parallel to the layers of the donor, within which pairs of $[CuCl_4]^{2-}$ anions are connected by hydrogen bonds through the two water molecules to form discrete units. The Cu−Cl bond lengths (average 2.25 Å) and angles (150°) are both quite normal for Cu(II) halides with a Jahn−Teller distortion. The bond lengths and angles of the three independent BEDT-TTF molecules are almost identical while the two different overlap modes are the same in each stack. (BEDT-TTF)$_3[CuCl_4]\cdot H_2O$ is the only BEDT-TTF salt with 3:2 charge stoichiometry that remains metallic down to very low temperatures at ambient pressure. Normally such salts undergo metal (or semimetal) to insulator (or semiconductor) transitions, some of which are sharp (e.g. (BEDT-TTF)$_3(ClO_4)_2$)[63] and others of which are broad (e.g. (BEDT-TTF)$_3Cl_2\cdot 2H_2O$).[64]

Being metallic down to at least 400 mK, (BEDT-TTF)$_3[CuCl_4]\cdot H_2O$ is a good prototype system to study the interaction between localized moments and conduction electrons, which is shown by two observations.[65] First, there is a shift in *g* value and broadening of the EPR line, the former being distinctly larger than those found in β- or α'-phase BEDT-TTF salts (2.003−2.010).[66] Second, at low temperature the spin susceptibility of the conduction electrons falls below its Pauli limit while that of the localized electrons increases. Most striking, however, the product of the spin susceptibility of the Cu resonance and the temperature rises at low temperature, indicating a short-range ferromagnetic interaction. Fitting the data to the Bleaney−Bowers[67] model indicates a ferromagnetic exchange constant of 4 K. Since the shortest Cu−Cu distance is 8.5 Å, the direct exchange interaction between the Cu moments should

be very small. On the other hand, the $[CuCl_4]^{2-}$ are arranged as dimers bridged by H_2O, which may provide an exchange pathway. Nor can we rule out the possibility that exchange between Cu moments is mediated by the free carriers of the BEDT-TTF layers (the RKKY mechanism).

While the interaction between the BEDT-TTF and the metal ion spins is weak yet observable in (BEDT-TTF)$_3$[CuCl$_4$]·H$_2$O, it is negligible in semiconducting (BEDT-TTF)$_2$[FeCl$_4$] and insulating (BEDT-TTF)-[FeBr$_4$].[47] By contrast, in (BEDT-TTF)$_3$[CuBr$_2$Cl$_2$] the interaction between the two sublattices is strong, and structural phase transitions transform the electrical and magnetic properties.[68] The crystal structures of the $[CuBr_4]^{2-}$ and $[CuCl_2Br_2]^{2-}$ salts are very different from the $[CuCl_4]^{2-}$ salt, and their electronic properties are unrelated. Whereas the $[CuCl_4]^{2-}$ form a flattened tetrahedron, as expected for Jahn−Teller d^9 ions, the anions in the bromo salts are square-planar. In fact, this is the first compound in which planar $[CuBr_4]^{2-}$ has been found.[69] Nevertheless, the stoichiometry of all three salts is 3:1. Two crystallographically independent BEDT-TTF molecules (X and Y) are found in the bromo compounds; from their bond lengths, the charges are defined as 0 and +1.[70] Both crystal structures consist of layers of BEDT-TTF, stacked in XYYXYY sequence in the α-phase mode of packing, separated by square-planar tetrahalogenocuprate(II) (Figure 14).

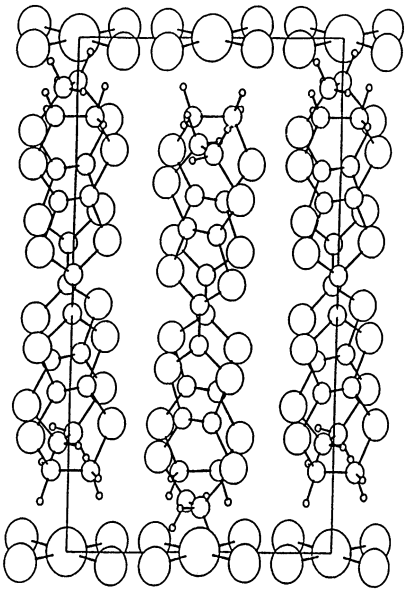

Figure 14. Layers of BEDT-TTF and $[CuBr_4]^{2-}$ in (BEDT-TTF)$_3$[CuBr$_4$]. (Reprinted with permission from ref 68. Copyright 1994 American Physical Society.)

The room temperature conductivities of the $[CuBr_4]^{2-}$ and $[CuCl_2Br_2]^{2-}$ salts are very similar, being low for metallic organic conductors and high for semiconductors, but they are affected dramatically by pressure,[68,71] showing the largest increase in conductivities with pressure of any known organic conducting solids: 25 S·cm^{-1}·kbar^{-1} up to 8 kbar, finally attaining a plateau at 22 kbar with 500 times the ambient pressure value. At low temperatures (59 K) there are phase transitions that take both salts from semimetallic to semiconducting at pressures above 3 kbar. Their magnetic properties are also unusual in that the susceptibility of the conduction electrons on the BEDT-TTF stacks is very high. The abrupt drop in susceptibility (Figure 15) at low temperature is due to the loss of the contribution from these electrons. To account for a contribution of this magnitude requires two spins per formula unit, which are antiferromagnetically coupled, suggesting that the $[CuBr_4]^{2-}$ and $[CuCl_2Br_2]^{2-}$ salts are just on the insulator side of the Mott−Hubbard transition. In such a case, semiconducting behavior is not due to a gap in the one-electron density of states but arises because the holes on the BEDT-TTF stacks localize due to the strong Coulomb interaction. The 3:2 charge stoichiometry of these salts requires two holes per three BEDT-TTF sites, and as noted above, the bond lengths show that two of the BEDT-TTF molecules are charged and that one is neutral. The transport properties are therefore those of a "magnetic" semiconductor, with an activation energy $U_{eff}/2$, where U_{eff} is the on-site Coulomb energy associated with the transfer of a charge to place two charges on a single site.

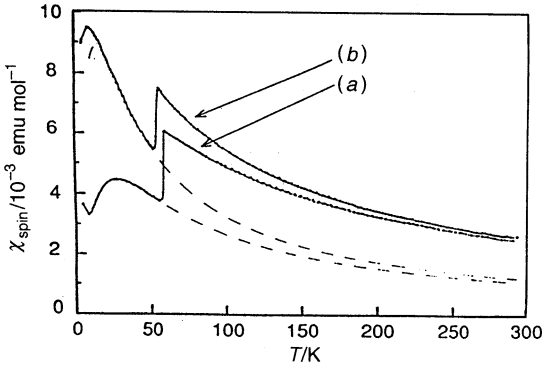

Figure 15. Magnetic susceptibilities of (BEDT-TTF)$_3$-[CuBr$_2$X$_2$]: (a) X = Br; (b) X = Cl. The dashed lines are fits to the quadratic layer Heisenberg antiferromagnetic model. (Reprinted with permission from ref 68. Copyright 1994 American Physical Society.)

In contrast to metallic (BEDT-TTF)$_3$[CuCl$_4$]·H$_2$O, only a single EPR line is seen in the bromo salts, though the g values above the 55−60 K transition are intermediate between those expected for a Cu(II) moment and for spins on BEDT-TTF sites. Hence, the two spin systems interact significantly, in contrast to the other magnetic anion salts.[47,62] The antiferromagnetic transition in (BEDT-TTF)$_3$[CuBr$_4$] has also been confirmed by solid-state proton NMR,[72] in which T_1^{-1} shows a divergent anomaly at 8 K that is still present under high pressure (about 10 K at 9 kbar) when the compound is metallic. The latter shows that the localized Cu^{2+} moments are still present when the lattice is metallic. An isostructural compound containing $NiCl_4^{2-}$ has also been reported. In contrast to the Cu salt, it has a metal−insulator transition at 100 K.[73]

Among other tetrabromocuprate(II) salts of derivatives of TTF, (TTM-TTF)CuBr$_4$ (tetramethylthio-TTF) contains $(TTM\text{-}TTF)^{2+}$ that are very strongly distorted away from planar and a linear Br···C···S···Br network.[74] As expected for a compound containing a +2 donor cation, this salt is a good

insulator and a Curie−Weiss paramagnet with a Weiss constant less than 1 K.

3.1.2. Hexahalo Anions

Although quite a number of charge-transfer salts containing organo-chalcogen donor cations have been prepared with hexahalo anions which are diamagnetic, such as $[PtCl_6]^{2-}$, $[SnCl_6]^{2-}$, and so forth,[75] rather few have been reported with paramagnetic anions (see Table 2). In fact, the only examples appear to be α-(BEDT-TTF)$_4$[ReCl$_6$]·C$_6$H$_5$CN,[76] (BEDT-TTF)$_2$[IrCl$_6$],[56] and a salt of dibenzo-TTF with $ReCl_6^{2-}$.[77] They are semiconductors, and the magnetic properties are dominated by the paramagnetism of the anions. Nevertheless, they present a number of interesting structural features.

The structure of α-(BEDT-TTF)$_4$[ReCl$_6$]·C$_6$H$_5$CN contains alternate layers of BEDT-TTF and [ReCl$_6$]·C$_6$H$_5$CN. The donor layers consist of two crystallographically independent stacks, in one of which the BEDT-TTF all carry a charge of +1 while in the other they are all neutral. Correspondingly, in the anion layers are rows of $[ReCl_6]^{2-}$ alternating with rows of C$_6$H$_5$CN. Interaction between the cation and anion layers appears to be determined largely by Coulomb forces, since the stacks of $(BEDT\text{-}TTF)^+$ are adjacent to the $[ReCl_6]^{2-}$ while the $(BEDT\text{-}TTF)^0$ are closest to the neutral solvent molecules. The compound is a semiconductor with an activation energy that varies slightly with temperature and a relatively high room temperature conductivity (3 S·cm^{-1} parallel to the layers and about 10 times less in the perpendicular direction). The low-temperature magnetic properties are dominated by the Curie−Weiss behavior of the anion, but at higher temperatures a component due to the BEDT-TTF is apparent. The latter was fitted successfully by a Heisenberg antiferromagnetic alternating chain model with $J_1/k = -16$ K and $J_2/k = -13$ K (Figure 16).

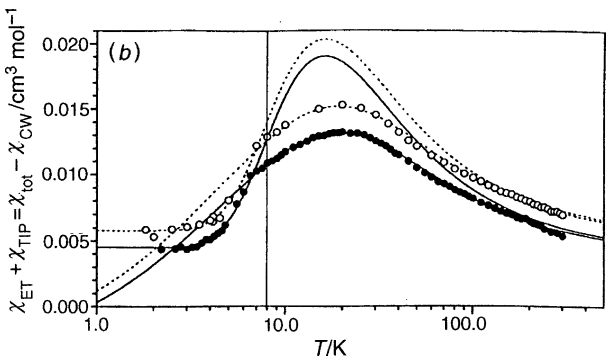

Figure 16. Susceptibility due to BEDT-TTF in α-(BEDT-TTF)$_4$[ReCl$_6$]·C$_6$H$_5$CN at 250 G (open circles) and 1000 G (filled circles). The data are fitted to the alternating chain AF model ($T > 8$ K) and the Bleaney−Bowers dimer model ($T < 8$ K). (Reprinted with permission from ref 76. Copyright 1997 Royal Society of Chemistry.)

Despite being electrocrystallized under the same conditions, the $IrCl_6^{2-}$ salt of BEDT-TTF has a completely different structure from that of the $ReCl_6^{2-}$ one.[54] It contains no solvent of crystallization; neither are there discrete layers of anions and cations. Instead there are face-to-face dimers of BEDT-TTF forming a three-dimensional network through end-to-end contacts, a relatively rare feature in BEDT-TTF charge-transfer salts. Despite this, the compound is a semiconductor with a room temperature conductivity of 10^{-2} S·cm^{-1}, a fact that is explained by its formulation as $(BEDT\text{-}TTF^+)_2[IrCl_6]^{2-}$, rather than the alternative $(BEDT\text{-}TTF^{1.5+})_2[IrCl_6]^{3-}$. The formulation as an Ir^{IV} salt is confirmed by the $S = {}^1/_2$ Curie−Weiss magnetic behavior of the anion, combined with an exceptionally high intradimer exchange constant of 965 K, fitted with the Bleaney−Bowers model.[67]

3.1.3. Pseudohalide-Containing Anions

Apart from the high-symmetry octahedral and tetrahedral halogeno complexes of transition metals, a variety of other monomeric anions have been incorporated into charge-transfer salts of TTF and its derivatives, in the search for combinations of conducting and magnetic properties. Some are complexes of pseudo-halide ligands such as CN^- and NCS^-, while others are of lower symmetry with mixed ligands (see Table 3). Among the latter are the first examples of long-range ferrimagnetic order in an organic−inorganic charge-transfer salt presented in section 5, where one of the sublattices is furnished by the pπ electrons of a molecular radical cation and the other by the d electrons of the transition metal complex anions. In a number of cases, the anions have been designed specifically to promote interaction between the organic and inorganic components of the lattice by building into them S atoms of the molecular donor.

The first hexacyanometalate salt of TTF was formulated as (TTF)$_{11}$[Fe(CN)$_6$]$_3$·5H$_2$O, an unusual stoichiometry that indicates a particularly complex structure.[78] Eight of the TTF are present in dimerized stacks and are assigned a charge of +1 from the bond lengths. The remaining ones have their molecular planes perpendicular to the stacks, two being neutral and the remaining one +1. Close contacts are indeed found between the $[Fe(CN)_6]^{3-}$ and the TTF (N···S 3.09 Å), but there is no report of cooperative magnetic properties, though the compound is a semiconductor. In contrast, BEDT-TTF salts with $[M(CN)_6]^{3-}$ (M = Fe, Co, Cr) have more conventional structures with alternating layers of cations and anions. Thus, (BEDT-TTF)$_5$[M(CN)$_6$]·10H$_2$O (M = Fe, Co) have the β-packing mode, albeit with a pentamer rather than the more usual tetrameter repeat unit.[79] Both compounds are semiconductors, although apparently there is appreciable Pauli paramagnetism in the Co salt, suggesting the presence of conduction electrons. A further series, (BEDT-TTF)$_4$(NEt$_4$)[M(CN)$_6$]·3H$_2$O (M = Fe, Co, Cr) has a κ-packing mode, and at room temperature all the BEDT-TTF have the same charge of +0.5, as found in the superconducting salts with the diamagnetic anions I_3^-, $Cu(NCS)_2^-$, and so forth.[80] Nevertheless, they are reported to be semiconducting in the neighborhood of room temperature. The magnetic susceptibility corresponds to the sum of contributions from the paramagnetic $[Fe(CN)_6]^{3-}$ and the organic sublattice, with no evidence for interaction between them. At 140 K, a sharp drop in susceptibil-

Table 3. Structures and Physical Properties of Charge-Transfer Salts Containing Pseudohalide Complex Anions

compound	packing	electrical properties	magnetic properties[a]	ref
$(TTF)_{11}[Fe(CN)_6]_3 \cdot 5H_2O$	dimerized stacks orthogonal monomers	semiconductor ($\sigma_{RT} \approx 10^{-3}$ S·cm^{-1})		78
$(BEDT\text{-}TTF)_5[Fe(CN)_6] \cdot 10H_2O$	β-donor packing; pentamers	semiconductor ($\sigma_{RT} \approx 0.02$ S·cm^{-1})	PM	79
$(BEDT\text{-}TTF)_5[Co(CN)_6] \cdot 10H_2O$	β-donor packing; pentamers	semiconductor ($\sigma_{RT} \approx 0.5$ S·cm^{-1})	Pauli paramagnet	79
$(BEDT\text{-}TTF)_4NEt_4[Fe(CN)_6] \cdot 3H_2O$	κ-donor layers	semiconductor ($\sigma_{RT} \approx 0.2$ S·cm^{-1})	PM; $C = 1.3$ emu·K·mol^{-1}	79
$(BEDT\text{-}TTF)_4NEt_4[Co(CN)_6] \cdot 3H_2O$	κ-donor layers	semiconductor ($\sigma_{RT} \approx 10$ S·cm^{-1})	PM	79
$(BEDT\text{-}TTF)_4NEt_4[Cr(CN)_6] \cdot 3H_2O$	κ-donor layers	semiconductor ($\sigma_{RT} \approx 0.15$ S·cm^{-1})	PM	79
$(BEST)_4[Fe(CN)_6]$	β-donor packing	semiconductor ($\sigma_{RT} \approx 11$ S·cm^{-1}; $E_a = 0.025$ eV)	PM	81, 82
$(BEST)_3[Fe(CN)_6]2 \cdot H_2O$	interpenetrated layers of cations 2+ and anions	semiconductor ($\sigma_{RT} \approx 10^{-6}$ S·cm^{-1})	PM	81, 82
$(BET\text{-}TTF)_4(NEt_4)_2[Fe(CN)_6]$	κ-donor layers	semiconductor ($\sigma_{RT} \approx 11.6$ S·cm^{-1}; $E_a = 0.045$ eV)	PM	82
$(BEDT\text{-}TTF)_2Cs[Co(NCS)_4]$	α-donor layers	metal−insulator transition at 20 K ($\sigma_{RT} = 14$ S·cm^{-1})		83
$(BEDT\text{-}TTF)_4[Cr(NCS)_6] \cdot PhCN$	α-donor layers	semiconductor ($\sigma_{RT} \approx 5 \times 10^{-3}$ S·cm^{-1}; $E_a = 0.26$ eV)	PM	86, 87
$(BEDT\text{-}TTF)_5NEt_4[Cr(NCS)_6] \cdot THF$	β-donor layers	semiconductor ($\sigma_{RT} \approx 10$ S·cm^{-1})	PM; $C =$ emu·K·mol^{-1}; $\lvert D \rvert = 7.3$ cm^{-1}	86, 88
$(BEDT\text{-}TTF)_5[Cr(NCS)_6] \cdot (DMF)_4$	β-donor layers	semiconductor ($\sigma_{RT} \approx 5$ S·cm^{-1})	PM; $\lvert D \rvert = 2.8$ cm^{-1}	88
$(BEDT\text{-}TTF)_{5.5}[Cr(NCS)_6]$	β-donor layers	semiconductor ($\sigma_{RT} \approx 2$ S·cm^{-1}; $E_a = 0.03$ eV)	PM; $\lvert D \rvert = 4.7$ cm^{-1}	87, 88
$(BEDT\text{-}TTF)_4[Fe(NCS)_6] \cdot CH_2Cl_2$	cation and anion layers	semiconductor ($\sigma_{RT} = 7 \times 10^{-3}$ S·cm^{-1}; $E_a = 0.7$ eV)	PM; $C = 4.926$ emu·K·mol^{-1}; $\theta = -0.19$ K	89
$(BEDT\text{-}TTF)_4[Fe(NCS)_6] \cdot (pip)$	orthogonal dimers/monomers	semiconductor ($\sigma_{RT} = 4.2$ S·cm^{-1}; $E_a = 0.25$ eV)		90
$(BEDT\text{-}TTF)_5NEt_4[Fe(NCS)_6]$	β-donor layers	semiconductor ($\sigma_{RT} = 4.0$ S·cm^{-1}; $E_a = 0.03$ eV)		90
$(BMDT\text{-}TTF)_4[Cr(NCS)_6]$		-		91
$(BEDT\text{-}TTF)_2[Cr(NCS)_4(NH_3)_2]$	dimerized, donor layers; anion layers	semiconductor ($\sigma_{RT} = 30$ S·cm^{-1}; $E_a = 0.056$ eV)	PM	89
$(BEDT\text{-}TTF)_2[Cr(NCS)_4\text{-}bipym] \cdot 25H_2O$	no π-stacking of anions and cations	semiconductor ($\sigma_{RT} = 0.015$ S·cm^{-1}; $E_a = 0.3$ eV)	PM; $C = 1.82$ emu·K·mol^{-1}; $\theta = -0.26$ K	124
$(TMTTF)[Cr(NCS)_4phen]$	donor dimers	insulator	AFM; TN = 3.0 K	126
$(TMTSF)_3[Cr(NCS)_4phen]$	no close cation−anion contacts	semiconductor ($\sigma_{RT} = 0.022$ S·cm^{-1}; $E_a = 0.16$ eV)	PM; $C = 3.57$ emu·K·mol^{-1}; $\theta = -3.82$ K	126

[a] PM = paramagnetic; AFM = antiferromagnetic.

ity arises from a charge disproportion among the dimers in the κ-structure, so that one consists of BEDT-TTF$^+$ and another of neutral molecules. The spin susceptibility measured by EPR confirms the presence of the same transition in the isostructural salt with diamagnetic $[Co(CN)_6]^{3-}$ as anion, indicating further that the anion plays only a minor role.[79]

Three different salts of $[Fe(CN)6]^{3-}$ with the organic donors BEST-TTF and BET-TTF (Chart 1) have also been reported: β-$(BEST\text{-}TTF)_4[Fe(CN)_6]$, $(BEST\text{-}TTF)_3[Fe(CN)_6]_2.H_2O$, and κ−$(BET\text{-}TTF)_4(NEt_4)_2[Fe(CN)_6]$.[81,82] In the 3:2 phase the structure shows an unusual interpenetration of the donor molecules and the anions. This fact may be due to the +2 charge of BEST-TTF (very unusual in any TTF-type donor and unprecedented with BEST-TTF). The magnetic properties of this salt correspond to the paramagnetic $[Fe(CN)_6]^{3-}$ anions, as the organic sublattice does not contribute. The 4:1 salt of the BET-TTF donor presents the typical alternating layers of anions and donors. The organic layers are formed by only one BET-TTF molecule, with a charge of $^1/_4$, packed in a κ-phase. The room temperature conductivity is very high (11.6 S·cm^{-1}), although the thermal behavior shows that this salt is a semiconductor with a low activation energy of 0.045 eV. The high electron delocalization of this salt is confirmed by the ESR studies on a single crystal that show a

Dysonian line when the magnetic field is parallel to the organic layers.[82]

Because specific nonbonding interactions between chalcogen atoms in neighboring molecules are such a common feature of the solid state chemistry of the group 16 elements, one strategy for promoting interaction between cation and anion sublattices in TTF-type charge-transfer salts is to incorporate group 16 atoms in the anion, preferably in a terminal position. The most convenient ligand for this purpose is NCS^-, which fortunately is bound to most transition metals through N. A salt of BEDT-TTF with tetrahedral $[Co(NCS)_4]^{2-}$ has the α-packing motif[83] and is isostructural with the series of α-$(BEDT\text{-}TTF)_2M[Hg(SCN)_4]$ (M = NH_4, K, Rb), which has been much studied by physicists because of the interplay between superconducting and antiferromagnetic ground states.[84,85] Nevertheless, the compound α-$(BEDT\text{-}TTF)_2Cs[Co(NCS)_4]$ is a metal but undergoes a metal−insulator transition at 20 K, and in the crystal structure there are no close BEDT-TTF···SCN contacts. Such contacts are indeed found in the several salts of BEDT-TTF prepared with the paramagnetic anions $[Cr(NCS)_6]^{3-}$ and $[Fe(NCS)_6]^{3-}$. With the Cr(III) anion a 4:1 phase—$(BEDT\text{-}TTF)_4[Cr(NCS)6]\cdot PhCN$—two 5:1 phases—β-$(BEDT\text{-}TTF)_5[Cr(NCS)_6](DMF)_4$ and β-$(BEDT\text{-}TTF)_5(NEt_4)\cdot[Cr(NCS)_6](THF)$—and a 5.5:1 phase—β-$(BEDT\text{-}TTF)_{5.5}[Cr(NCS)_6]$—have been prepared. Curiously, this last phase is closely related to the two other 5:1 phases, since the extra half BEDT-TTF molecule is located in the anion layer, replacing the solvent molecules of the other 5:1 phases.[86] All these salts are semiconductors with high room temperature conductivities in the range 1−10 $S\cdot cm^{-1}$. The magnetic properties correspond to the sum of both sublattices with zero field splittings in the range 3−10.5 K in the Cr(III) ion.[87,88] With the Fe(III) anion, two 4:1 phases—$(BEDT\text{-}TTF)_4[Fe(NCS)_6]\cdot CH_2Cl_2$[89] and $(BEDT\text{-}TTF)_4[Fe(NCS)_6]\cdot$(piperidine)[90]—and one 5:1 phase—$(BEDT\text{-}TTF)_5(NEt_4)[Fe(NCS)_6]$[90]—have been prepared. The Cr(III) anion has also been used with the bis(methylene)dithio-TTF (BMDT-TTF) donor in the salt $(BMDT\text{-}TTF)_4[Cr(NCS)_6]$. Most of these salts present short anion−cation S···S contacts despite having a layer structure with alternating anions and cations because one of the NCS groups penetrates into the cation layer. There are also close contacts between NCS groups on neighboring anions, but despite these features the Fe(III) compounds remain paramagnetic to 1.5 K (as the Cr(III) salts) with only a very small Weiss constant (−0.19 K in the $(BEDT\text{-}TTF)_4[Fe(NCS)_6]\cdot CH_2Cl_2$ salt).

3.2. Polynuclear Metal Complexes

One strategy for exploring the subtle structure−property relationships in molecular charge-transfer salts by chemical means is to compare isostructural and isosymmetrical series. Furthermore, formation of solid solutions could also help to achieve systematic variations of structure and properties, for which purpose it is of interest to identify anion types that facilitate chemical doping. In this respect, polynuclear metal complexes show promise in forming extended isostructural series with TTF and BEDT-TTF. The anion size may be finely tuned by substituting the terminal and capping groups, and in addition, different solvent molecules may nest in the cavities between the cluster anions without greatly altering the structure of the anion layer. Finally, these salts are promising candidates for testing the feasibility of anion layer doping, since the effects of structural and electrostatic disorder are expected to be small when the dopant is embedded within a thick anion layer. Potential doping mechanisms include mixed solvents (with the additional possibility of including cations or anions in the cavity between the clusters) and mixed anions.

3.2.1. Dimeric Anions

In the quest for compounds exhibiting magnetic exchange interactions between metal ions situated within the anion layers, it is logical to look for groups that will bridge neighboring metal centers and transmit superexchange between them. Ambidentate ligands such as NCS^- and $(C_2O_4)^{2-}$ are simple examples, and we begin by mentioning a few charge-transfer salts in which these ligands bridge discrete pairs of metals.

The anion $[Fe_2(C_2O_4)_5]^{4-}$, which contains high spin Fe^{III} ions bridged by one $C_2O_4^{2-}$, has been incorporated in TTF,[92] TMTTF,[92] and BEDT-TTF[93] salts. In every case the magnetic behavior is dominated by the magnetic anion. In the TTF salt, which has the stoichiometry $(TTF)_5[Fe_2(C_2O_4)_5]\cdot 2PhMe\cdot 2H_2O$, there are chains of donors surrounded by the dimeric anions and orthogonal TTF dimers, while, in the salt $(TMTTF)_4[Fe_2(C_2O_4)_5]\cdot PhCN\cdot 4H_2O$, there are segregated stacks of donors and anions in a "checkerboard" arrangement. During the synthesis of the above TTF salt, another salt with the trisoxalatoferrate anion is also formed. It is a 7:2 phase formulated as $(TTF)_7[Fe(C_2O_4)_3]_2\cdot 4H_2O$, where the TTFs are packed in chains surrounded by four orthogonal dimers of TTF molecules and four paramagnetic $[Fe(C_2O_4)]^{3-}$ anions.[92] In the salt $(BEDT\text{-}TTF)_4[Fe_2(C_2O_4)_5]$, there are closely spaced cation dimers, so that the overall structure resembles the "checkerboard" arrangement found in $(BEDT\text{-}TTF)_2[Ge(C_2O_4)_3]\cdot C_6H_5CN$.[94] The dimers of spin-paired monopositive cations therefore do not contribute to the magnetic properties; neither are there layers of alternating anions and cations. In all these salts, the antiferromagnetic exchange between the Fe^{III} is quite comparable in magnitude to that found in other oxalate-bridged Fe^{III} dimers.

Likewise, some salts containing oxalate-bridged dimeric anions are $(BEDT\text{-}TTF)_5[MM'(C_2O_4)(NCS)_8]$ where MM′ is either CrFe or CrCr.[95] Here the presence of NCS^- is especially noteworthy because of the opportunity it presents for cation−anion S···S interactions. The latter compound does have a layer lattice of alternating cations and anions, the former being related to (but crucially different from) the κ-arrangement of orthogonal dimers. In this case the dimers are interleaved by monomers, which are assigned charges close to zero by band structure calculations. In agreement with those calculations, the compounds are semiconductors, albeit with rela-

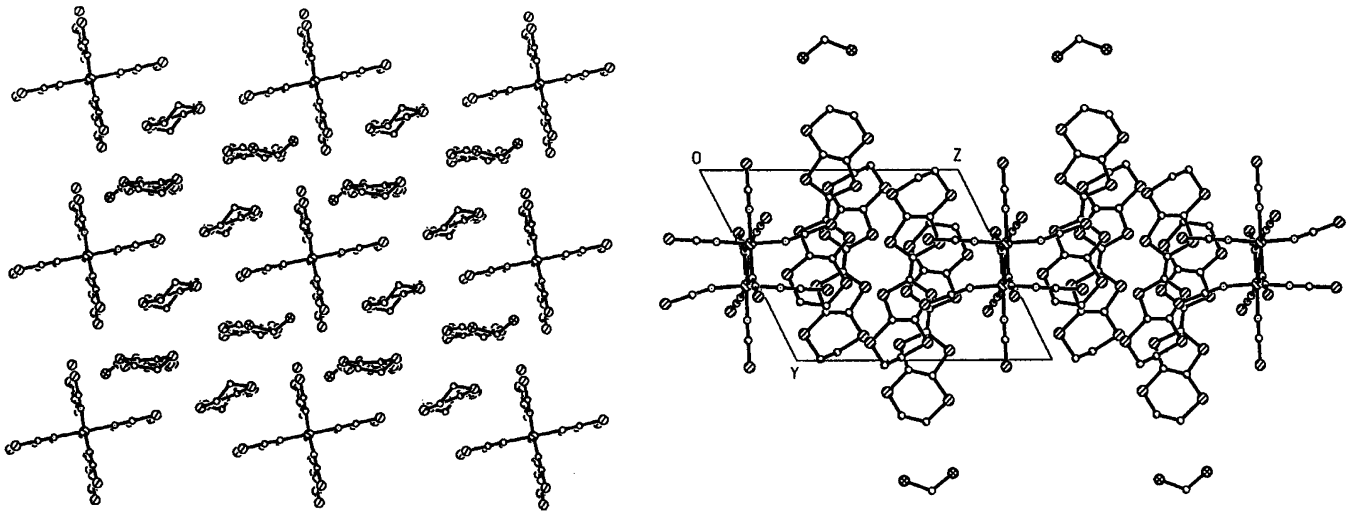

Figure 17. Crystal structure of $(BEDT\text{-}TTF)_3[Re_2(NCS)_{10}]\cdot 2CH_2Cl_2$: (left) along the BEDT-TTF long axes; (right) along the *a*-axis. (Reprinted with permission from ref 98. Copyright 1997 American Chemical Society.)

tively high room temperature conductivity and low activation energy. From the standpoint of magnetism, the principal feature of interest is a ferromagnetic intradimer exchange interaction in the CrFe compound, leading to the $S = 4$ dimer ground-state expected for $S = {}^3/_2$ (Cr) and ${}^5/_2$ (Fe). For the CrCr anion a metallic 8:1 phase with BEDT-TTF has also been reported: $(BEDT\text{-}TTF)_8[Cr_2(C_2O_4)(NCS)_8]$.[96] The room temperature conductivity for this salt is 0.1 $S\cdot cm^{-1}$ and increases with decreasing temperature to reach a value of 1 $S\cdot cm^{-1}$ at 180 K.[96] The magnetic properties are dominated by the antiferromagnetic behavior of the Cr−Cr dimer, as in the 5:1 phase.

Dimeric anions containing only NCS^- were first synthesized many years ago in the form of $[Re_2(NCS)_{10}]^{n-}$ ($n = 2, 3$).[97] The structures of their BEDT-TTF salts are quite different, although the anions themselves only vary slightly in geometry with changing charge.[98] The structure of the $n = 3$ compound consists of layers containing both cations and anions with several very short S···S contacts between them but no continuous network of closely interacting BEDT-TTF (Figure 17). The total susceptibility is modeled best as the sum of Curie−Weiss and dimer contributions, the former attributed to the anions and the latter to one of the cations, whose spin remains impaired while those of the remaining two cations in the unit cell are paired.

A special case of a dimeric anion appears in the semiconducting salts $(TTF)_2[Fe(tdas)_2]$ and $(BEDT\text{-}TTF)_2[Fe(tdas)_2]$ (tdas = 1,2,5-thiadiazole-3,4-dithiolate). The structures of both salts show the typical layered structure with dimerized chains in the anionic layer and β or α packings in the TTF[99] and BEDT-TTF[100] salts, respectively. Both salts are semiconductors with room temperature conductivities of 0.03 and 1 $S\cdot cm^{-1}$ and activation energies of 0.18 and 0.10 eV, respectively. Due to the dimerization of the $[Fe(tdas)_2]^{2-}$ anions, the Fe(III) ion has a square-pyramidal coordination. Therefore, it has a $S = {}^3/_2$ ground spin state, as has been confirmed by magnetic measurements and Mössbauer spectroscopy in the NBu_4^+ salt of this anion.[101,102] The magnetic data for both salts are consistent with the formation of antiferromagnetic dimers ($J/k = -154$ K for the TTF salt and −99 K for the BEDT-TTF salt). In the BEDT-TTF salt besides the contribution of the Fe(III) dimers, there is a magnetic contribution from the BEDT-TTF molecules that have been reproduced with a model of interacting antiferromagnetic $S = {}^1/_2$ chains.[100] There is also a 3:2 TTF salt with this anion, although the structure is not known and the magnetic properties show a Curie type behavior, suggesting that in this case the anions are not dimerized.[103]

3.2.2. Polyoxometalate Clusters

Polyoxometalates (POMs) have been found to be extremely versatile inorganic building blocks for constructing organic/inorganic molecular materials with unusual electronic properties. General reviews that provide a perspective of the use of POMs in this area can be found in ref 104. In the context of the present review, these bulky metal-oxide clusters possess several characteristics that have made them suitable and attractive as magnetic counterions for new TTF-type radical salts in which localized and delocalized electrons can coexist: they are anions that can be rendered soluble in polar organic solvents; they can incorporate one or more magnetically active transition metal ions at specific sites within the cluster; and their molecular properties, such as charge, shape, and size, can be easily varied. In particular, it is possible to vary the anionic charge while maintaining the structure of the POM.

A drawback of these bulky anions is that, although they often stabilize unusual new packing arrangements of the organic ions, their high charges tend to localize the charges of the organic sublattice, making it difficult to achieve high electrical conductivities and metallic behaviors for these materials. All the known radical salts with magnetic POMs are based on the organic donor BEDT-TTF. The POMs used to prepare these materials are depicted in Figure 18. The magnetic and electrical properties of these materials are summarized in Table 4.

3.2.2.1. Keggin Anions. α-Keggin anions of the type $[X^{n+}W_{12}O_{40}]^{(8-n)-}$ (abbreviated as $[XW_{12}]$; Figure

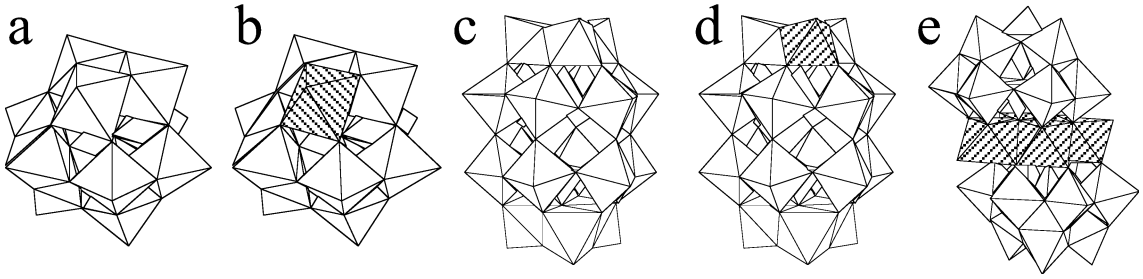

Figure 18. Types of magnetic polyoxometalates used as inorganic counterions for BEDT-TTF-type radical salts: (a) nonsubstituted α-Keggin anions $[X^{n+}W_{12}O_{40}]^{(8-n)-}$ (X = Cu^{II}, Co^{II}, Fe^{III}, ...); (b) monosubstituted α-Keggin anions $[X^{n+}Z^{m+}(H_2O)M_{11}O_{39}]^{(12-n-m)-}$ (X = P^{V}, Si^{IV}; M = Mo^{VI}, W^{VI}; Z = Fe^{III}, Cr^{III}, Mn^{II}, Co^{II}, Ni^{II}, Cu^{II}); (c) the Dawson−Wells anion $[P_2W_{18}O_{62}]^{6-}$; (d) the monosubstituted Dawson−Wells anion $[ReOP_2W_{17}O_{61}]^{6-}$; (e) the magnetic anions $[M_4(PW_9O_{34})_2]^{10-}$ (M^{II} = Co, Mn).

Table 4. Structures and Physical Properties of BEDT-TTF Charge-Transfer Salts Containing Polyoxometalate Anions

compound	packing	electrical properties	magnetic properties	ref
$ET_8[MW_{12}O_{40}]$; M = Co^{II}, Cu^{II},Fe^{III}	layers of donors (α-packing) made of regular and dimerized stacks	semiconductors; σ_{RT} = 0.15−0.03 S·cm^{-1}; E_a = 0.094−0.159 eV	regular AF chains of BEDT-TTF (J = −60 cm^{-1}) alternating with dimerized AF chains (J = −310 cm^{-1}) in coexistence with paramagnetic metal ions	106
$ET_8[XW_{11}M(H_2O)O_{39}]$; M = Co^{II}, Cu^{II}, Ni^{II}, Fe^{III}, Cr^{III}; X = P^{III}, Si^{IV}	layers of donors (α-packing) made of regular and dimerized stacks	semiconductors; σ_{RT} = 0.15−0.03 S·cm^{-1}; E_a = 0.094−0.159 eV	regular AF chains of BEDT-TTF (J = −80 cm^{-1}) alternating with dimerized AF chains (J = −280 cm^{-1}) in coexistence with paramagnetic metal ions	108
$ET_8[PM_{11}Mn(H_2O)O_{39}]$; M = W, Mo	layers of donors (α-packing) made of regular and dimerized stacks; chains of polyoxometalates	semiconductors; σ_{RT} = 0.1 S·cm^{-1}; E_a ∼ 100 meV	regular AF chains of BEDT-TTF alternating with dimerized AF chains in coexistence with paramagnetic manganese(II) ions	108
$ET_{11}[ReOP_2W_{17}O_{61}]$	layers of donors (β-packing)	metallic; σ_{RT} = 11.8 S·cm^{-1}; M−I transition at ≈200 K; E_a = 27 meV	paramagnetic behavior coming from non-interacting Re ions (S = 1/2)	109
$ET_6H_4[M_4(PW_9O_{34})_2]$; M = Co^{II}, Mn^{II}	unknown	insulator	the magnetic behavior corresponds to that of the ferromagnetic Co^{II} cluster or to the antiferromagnetic Mn^{II}cluster	111

18a) were first combined with BEDT-TTF molecules to provide an extensive series of radical salts having the general formula $(BEDT\text{-}TTF)_8[XW_{12}O_{40}](solv)_n$ (solv = H_2O, CH_3CN). Here, the central tetrahedral XO_4 site may contain a diamagnetic heteroatom ($2(H^+)$, Zn^{II}, B^{III}, and Si^{IV})[105,106] or a paramagnetic one (Cu^{II}, Co^{II}, Fe^{III}, ...).[106] The compounds crystallize in two closely related structure types, α_1 and α_2, consisting of alternating layers of BEDT-TTF molecules with an α-packing mode and the inorganic Keggin anions forming close-packed pseudohexagonal layers in the *ac*-plane (Figure 19). In the organic layers there are three (α_1 phase) or two (α_2 phase) crystallographically independent BEDT-TTF molecules which form two types of stacks: a dimerized chain and an eclipsed one. The shortest interchain S···S distances, ranging from 3.46 to 3.52 Å, are significantly shorter than the intrachain ones (from 3.86 to 4.04 Å), emphasizing the two-dimensional character of the packing. Another important feature of this structure is the presence of short contacts between the organic and the inorganic layers which take place between the S atoms of the eclipsed chains and some terminal O atoms of the polyoxoanions (3.15 Å), and via hydrogen bonds between the ethylene groups of the BEDT-TTF molecules and several O atoms of the anions (3.13 Å).

From the electronic point of view, an inhomogeneous charge distribution was found in the organic layer by Raman spectroscopy, in which the eclipsed chain is formed by almost completely ionized $(BEDT\text{-}TTF)^{\bullet+}$ ions, while the dimerized chain contains partially charged BEDT-TTFs. This charge distribution accounts for the electrical and magnetic properties of these salts. All of them exhibit semiconducting behavior ($\sigma_{RT} \approx 10^{-1}-10^{-2}$ S·cm^{-1} and $E_a \approx 100-150$ meV), independent of the charge in the organic sublattice (see inset in Figure 20). As far as the magnetic properties are concerned, the localized electrons in the eclipsed chain (one unpaired electron per BEDT-TTF) account for the chain antiferromagnetism, and the delocalized electrons in the mixed-valence dimeric chain account for the presence of an activated magnetic contribution at high temperatures and for a Curie tail contribution at low temperatures (Figure 20).

For those salts containing magnetic polyanions, the isolation of the magnetic center (situated in the

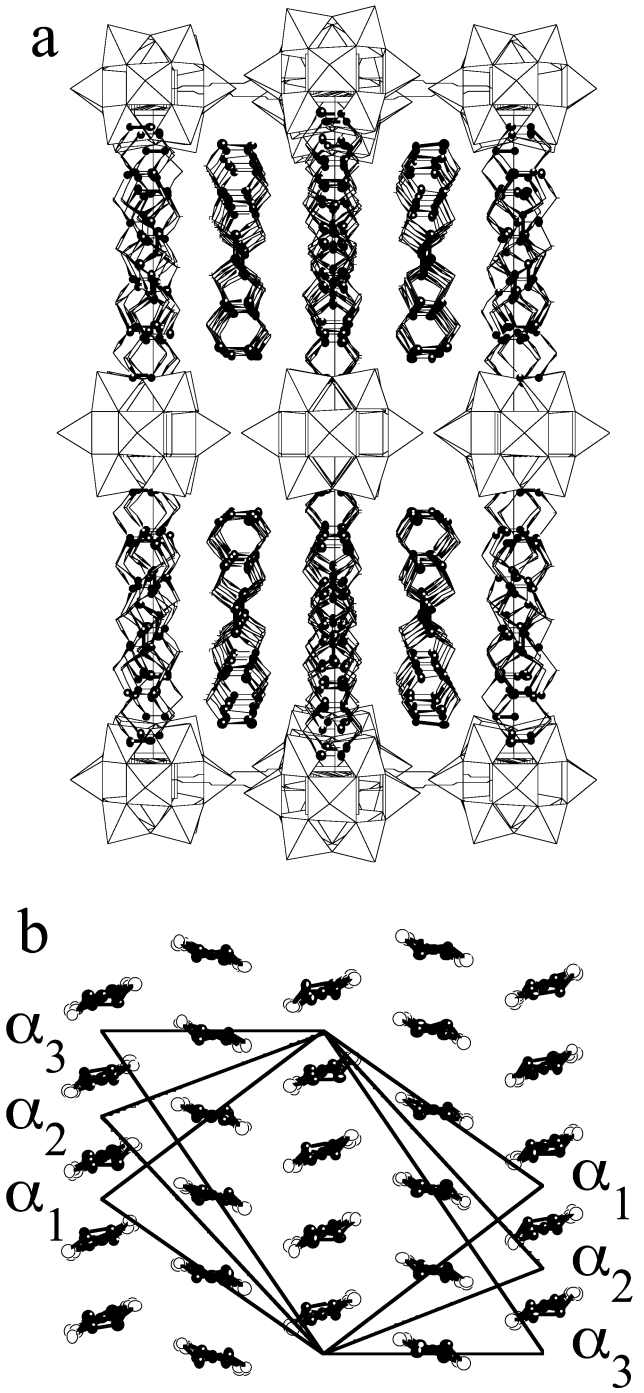

Figure 19. (a) Structure of the radical salts $(BEDT\text{-}TTF)_8[XW_{12}O_{40}]$ showing the layers of Keggin polyoxoanions and the two types of chains, eclipsed and dimerized, in the organic layers. (b) Projection of the organic layer showing the structural relationship between the three crystallographic α-phases. (Reprinted with permission from ref 106a. Copyright 1994 Wiley.)

central tetrahedral cavity of the Keggin structure) precludes any significant magnetic interaction with the organic spin-sublattice. In fact, the electron paramagnetic resonance (EPR) spectra show both the sharp signal of the radical cation and the signals associated with the paramagnetic metal ions. These salts represent the first examples of hybrid materials based on polyoxometalates in which *localized magnetic moments and itinerant electrons coexist in the two molecular networks*.

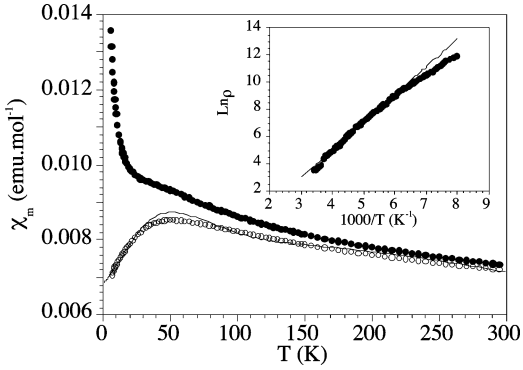

Figure 20. Plot of the magnetic susceptibility (χ_m) vs T for the $(BEDT\text{-}TTF)_8[BW_{12}O_{40}]$ radical salt (filled circles). Open circles correspond to the corrected magnetic susceptibility (after subtracting a paramagnetic Curie-type contribution). Solid lines represent the best fit to a model that assumes an antiferromagnetic Heisenberg chain behavior (with $J \sim -30$ cm^{-1}; the exchange Hamiltonian is written as $-2JS_iS_j$) for the eclipsed chain and an activated magnetic contribution (with $J \sim -150$ cm^{-1}) coming from the dimeric chain. Inset: Semilogaritmic plot of the electrical resistivity (Ω·cm) vs reciprocal temperature. (Reprinted with permission from ref 106a. Copyright 1994 Wiley.)

A salt containing the one-electron reduced polyoxometalate $[PMo_{12}O_{40}]^{4-}$ has also been reported.[107] It crystallizes in the α_1-structure, although some structural disorder has been found. From the electronic point of view, this compound may be of special interest, as it contains delocalized electrons in the mixed-valence inorganic sublattice. However, the magnetic properties of this compound, in particular, the EPR spectroscopy, indicate that the latter electrons do not interact with those of the organic sublattice.

With the aim of bringing the magnetic moments localized on the Keggin polyanions closer to the π electrons on the organic molecules, monosubstituted Keggin anions having one magnetic ion at the polyoxometalate surface have been used.[108] These are of the type $[X^{n+}Z^{m+}(H_2O)M_{11}O_{39}]^{(12-n-m)-}$ ($X = P^{V}$, Si^{IV}; $M = Mo^{VI}$, W^{VI}; $Z = Fe^{III}$, Cr^{III}, Mn^{II}, Co^{II}, Ni^{II}, Cu^{II}, and Zn^{II}) (abbreviated as $[XZM_{11}]$; Figure 18b). They can be considered as derived from the nonsubstituted Keggin anions $[X^{n+}M_{12}O_{40}]^{(8-n)-}$ by simply replacing one of the external constituent atoms and its terminal oxygen atom by a 3d transition metal atom, Z, and a water molecule, respectively. This series of semiconducting BEDT-TTF radical salts maintains the general stoichiometry (8:1) and the structural characteristics of the previous family. In fact, most of them crystallize in the α_2-structure ($Z = Fe^{III}$, Cr^{III}, Co^{II}, Ni^{II}, Cu^{II}, and Zn^{II}). However, an unexpected arrangement of the Keggin anions has been observed in the Mn derivatives $(BEDT\text{-}TTF)_8[PMn^{II}M_{11}]$ ($M =$ W, Mo). Here a related structure (namely α_3) has been found in which the BEDT-TTFs are packed in the same way as in the other two phases, while the Keggin units are linked through a bridging oxygen atom to give an unprecedented chain of Keggin anions that runs along the *c*-axis of the monoclinic cell (Figure 21). The organic stacking remains nearly unchanged for the three crystalline α-phases.

The magnetic properties of this series are similar to those observed in BEDT-TTF salts with nonsub-

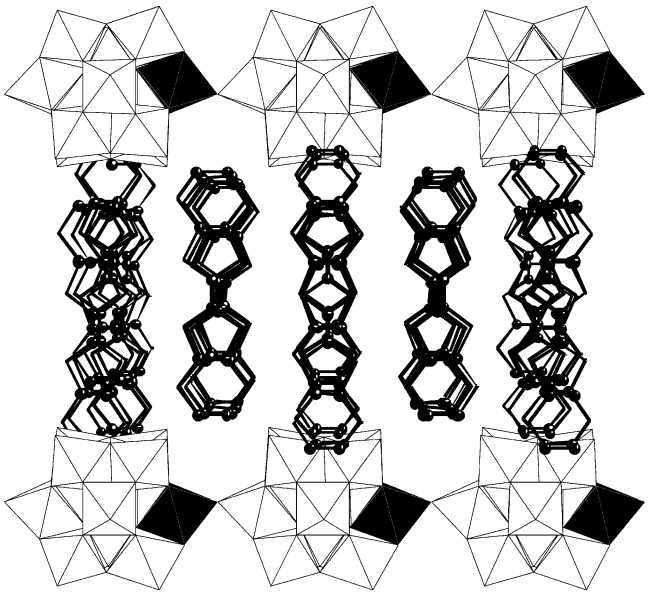

Figure 21. Structure of the $\{(BEDT\text{-}TTF)_8[PMnW_{11}O_{39}]\}_n$ radical salt showing the chains formed by the Keggin units. (Reprinted with permission from ref 108a. Copyright 1995 Wiley.)

stituted Keggin anions. No magnetic effects arising from the d−π interaction between these localized d electrons and the itinerant π electrons are detected down to 2 K, even though the two sublattices are closer than in the salts of the nonsubstituted Keggin anions. For example, in the Fe^{III} derivative, the magnetic behavior shows a decrease of the magnetic moment on cooling, which must be attributed, as before, to antiferromagnetic interactions in the organic sublattice, approaching the behavior of isolated paramagnetic metal ions at low temperature (Figure 22a). On the other hand, 4 K EPR measurements show signals characteristic of the two sublattices in all cases: a narrow signal at $g \approx 2$ with line width of 25−40 G arising from the BEDT-TTF radicals, plus broad signals that closely match those observed in the But4N^+ salts of the corresponding paramagnetic Keggin anions (Figure 22b).

3.2.2.2. The Dawson−Wells Anion $[P_2W_{18}O_{62}]^{6-}$. The Dawson−Wells anion $[P_2W_{18}O_{62}]^{6-}$ has also been used to prepare radical salts. In this anion 18 WO_6 octahedra share edges and corners, leaving two tetrahedral sites inside, which are occupied by P^V atoms. Its external appearance shows two belts of six octahedra capped by two groups of three octahedra sharing edges (Figure 18c). Electrochemical oxidation of BEDT-TTF in the presence of this polyanion leads to the new radical salt $(BEDT\text{-}TTF)_{11}[P_2W_{18}O_{62}]\cdot 3H_2O$.[109] The structure of this compound consists of layers of anions and BEDT-TTFs alternating in the *ac*-plane of the monoclinic cell (Figure 23a). Parallel chains of BEDT-TTF molecules form the structural arrangement of the organic layer. The organic molecules of neighboring chains are also parallel, leading to the so-called β-phase (Figure 23b). What is remarkable in this structure is the presence of six crystallographically independent BEDT-TTF molecules (noted as A, B, C, D, E, and F in Figure 23c) in such a way that each chain is formed by the repetition of groups of 11 BEDT-TTF molecules

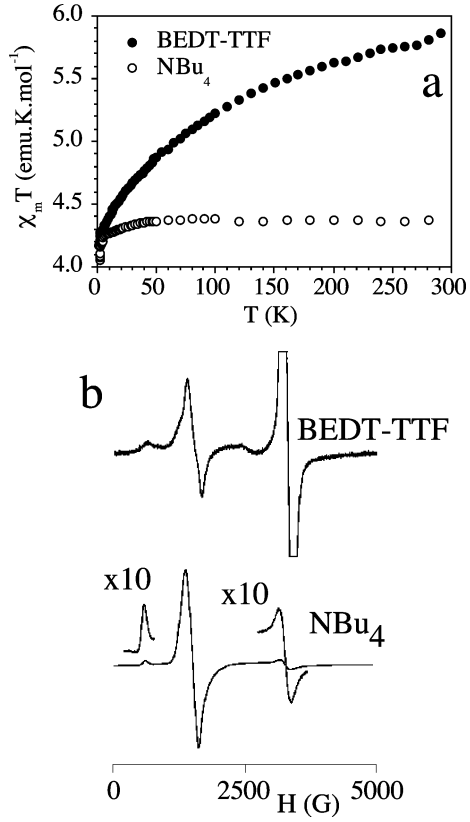

Figure 22. Magnetic properties of the $(BEDT\text{-}TTF)_8[SiFe^{III}(H_2O)Mo_{11}O_{39}]$ compared to the tetrabutylammonium (NBu_4) salt of the $[SiFe^{III}(H_2O)Mo_{11}O_{39}]^{5-}$ anion: (a) plot of the $\chi_m T$ product vs T; (b) comparison between the EPR spectra performed at 4 K. In the spectrum of the ET salt we observe the coexistence of the signal associated with the radical (sharp signal centered at 3360 G, $g = 2$) and the low field signals coming from the Fe^{III} ion (centered at 750 G ($g = 8.9$) and 1640 G ($g = 4.1$)). (Reprinted with permission from ref 108c. Copyright 1998 American Chemical Society.)

following the sequence ...ABCDEFEDCBA... stacked in a *exotic zigzag mode*. These unusual structural features illustrate the ability of polyoxometalates to create new kinds of packing in the organic component. But the most attractive characteristic of this salt concerns its electrical conductivity; it shows a *metallic-like behavior* in the region 230−300 K with an increase in the conductivity from ~5 $S\cdot cm^{-1}$ at room temperature to 5.5 $S\cdot cm^{-1}$ at 230 K. Below this temperature the salt becomes semiconducting, with a very low activation energy value of 0.013 eV (Figure 24a).

In view of this high conductivity, attempts have been made to prepare a related compound containing a magnetic center on the surface of the Dawson−Wells polyanion. As a result, a novel compound that contains a rhenium(VI) ion replacing a W in the Dawson−Wells structure has been obtained ($[ReOP_2W_{17}O_{61}]^{6-}$; Figure 18d). It is isostructural to the nonmagnetic one, and its electrical properties are also very close to those observed in that compound (Figure 24a). From the magnetic point of view, no evidence of interactions between the two electronic sublattices has been observed, despite the fact that there are strong intermolecular anion−cation contacts. In fact, the magnetic properties indicate the

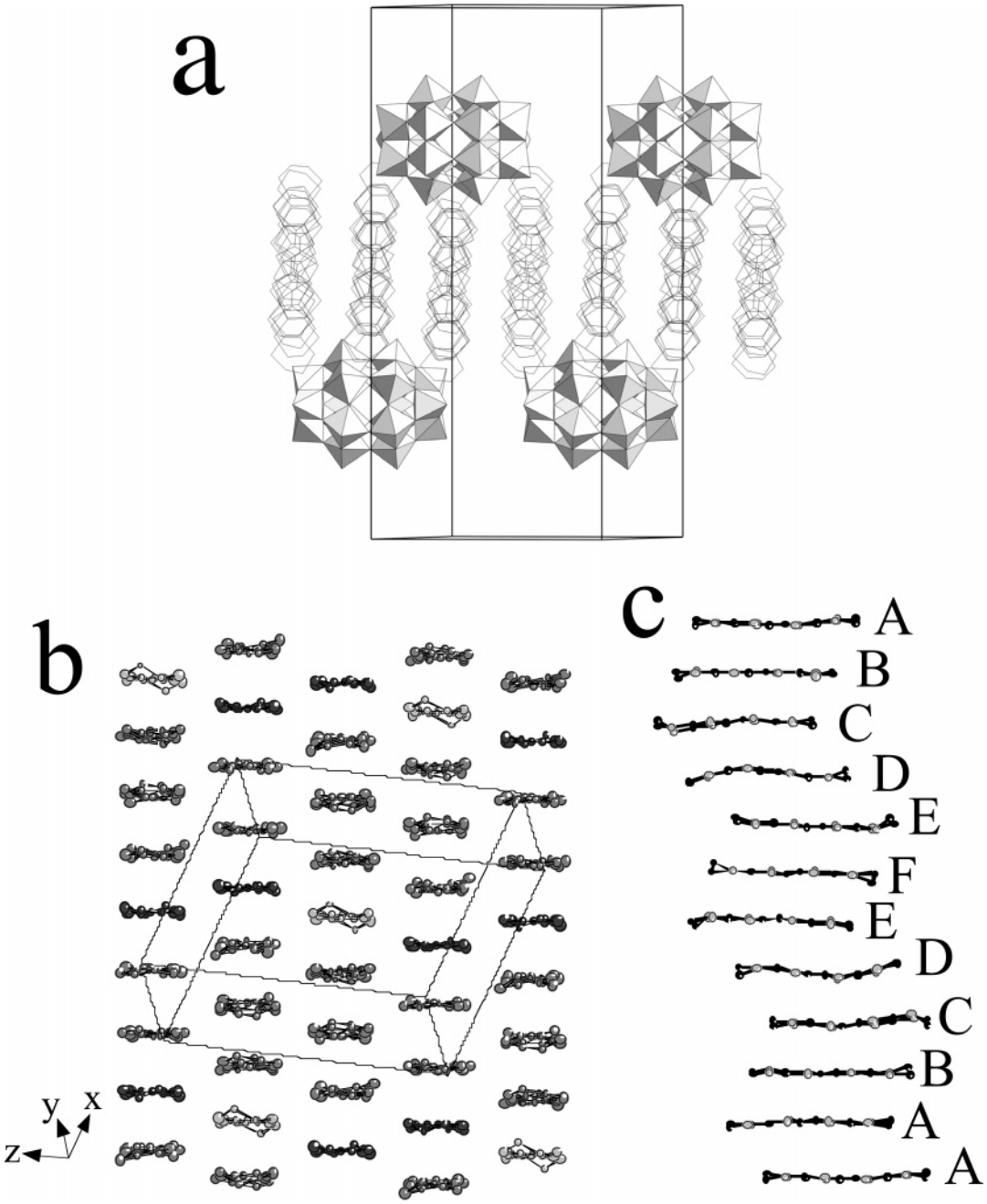

Figure 23. (a) Structure of the radical salt $(BEDT\text{-}TTF)_{11}[P_2W_{18}O_{62}]\cdot 3H_2O$ showing the alternating organic and inorganic layers. (b) View of the organic layer showing the β-packing mode. (c) View of the organic stacking showing the six different BEDT-TTFs (A−F). (Reprinted with permission from ref 109b. Copyright 2000 Royal Society of Chemistry.)

presence of the spin $S = {}^1/_2$ of the Re^{VI}, and EPR measurements show a spectrum very similar to that observed in the tetrabutylammonium salt of the polyoxometalate (Figure 24b). This novel compound constitutes an illustrative example of a hybrid salt showing *coexistence of a high electron delocalization with localized magnetic moments*.

3.2.2.3. The Magnetic Anions $[M_4(PW_9O_{34})_2]^{10-}$ ($M = Co^{2+}$, Mn^{2+}). Polyoxometalates of higher nuclearities have also been associated with organic donors. Thus, the magnetic polyoxoanions $[M_4(PW_9O_{34})_2]^{10-}$ (M^{2+} = Co, Mn), which have a metal nuclearity of 22, give black powders with TTF and crystalline solids with BEDT-TTF.[111] These polyoxoanions are of magnetic interest, since they contain a ferromagnetic Co_4 cluster or an antiferromagnetic Mn_4 cluster encapsulated between two polyoxotungstate moieties $[PW_9O_{34}]$ (See Figure 18e). This class of magnetic systems is currently being investigated, since polyoxometalate chemistry provides ideal examples of magnetic clusters of increasing nuclearities in which the exchange interaction phenomenon, as well as the interplay between electronic transfer and exchange, can be studied at the molecular level.[112]

The electrochemical oxidation of BEDT-TTF in the presence of these magnetic anions affords the isostructural crystalline materials $(BEDT\text{-}TTF)_6H_4[M_4(PW_9O_{34})_2]$, which have four protons to compensate the charge. The six BEDT-TTFs are completely charged (+1), and the compounds are insulators. The magnetic properties of these salts arise solely from the anions. No influence coming from the organic

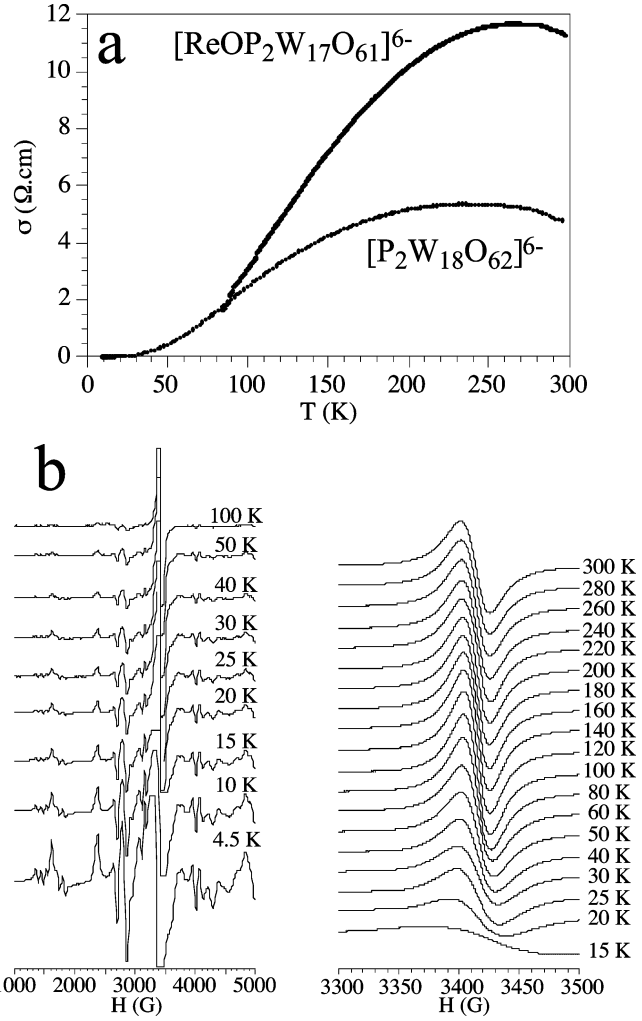

Figure 24. (a) Thermal variation of the dc electrical conductivity for $(BEDT\text{-}TTF)_{11}[P_2W_{18}O_{62}]\cdot 3H_2O$ and $(BEDT\text{-}TTF)_{11}[ReOP_2ReW_{17}O_{61}]\cdot 3H_2O$ showing the high conductivity at room temperature and the metallic behavior above 230 K. (b) EPR measurements at 4 K for the Re^{VI} derivative. (Reprinted with permission from ref 109b. Copyright 2000 Royal Society of Chemistry.)

component on the magnetic coupling within or among the clusters is detected down to 2 K. For example, in the Co derivative the χT product shows a sharp increase below 50 K upon cooling and a maximum at ~9 K, which is analogous to that observed in the K^+ salt and demonstrates that the ferromagnetic cluster is maintained when we change K^+ to $BEDT\text{-}TTF^+$. This also indicates a lack of interaction between the two components. This conclusion is supported by the EPR spectra performed at 4 K that show the same features for both salts: a very broad and anisotropic signal which extends from 1000 to 4000 G centered around 1620 G ($g = 4.1$) characteristic of the Co_4 cluster. No signal from the organic radical is observed, indicating a complete pairing of the spins of the $(BEDT\text{-}TTF)^+$ cations in the solid.

The two above compounds demonstrate the ability of the high nuclearity polyoxometalates $[M_4(PW_9O_{34})_2]^{10-}$ to form crystalline organic/inorganic radical salts with the BEDT-TTF donor. As such, they constitute the first known examples of hybrid materials containing a magnetic cluster and an organic donor.

To conclude this section, we can say that the combination of magnetic polyoxometalates with TTF-type organic donors has witnessed rapid progress in the past few years. This hybrid approach has provided a variety of examples of radical salts with coexistence of localized magnetic moments with itinerant electrons. This is the critical step toward the preparation of molecular materials combining useful magnetic and electrical properties. Thus far, however, the weak nature of the cation/anion contacts as well as the low conductivities exhibited by most of the reported materials have prevented the observation of an indirect interaction between the localized magnetic moments via the conducting electrons.

3.3. Chain Anions: Maleonitriledithiolates

Planar metallocomplex anions of the type metal−bisdichalcogenelene tend to form one-dimensional packings in the solid state when they are combined with the suitable cation. In the context of the molecular conductors, the metal−bismaleonitriledithiolates $[M(mnt)_2]^-$ (M(III) = Ni, Cu, Au, Pt, Pd, Co, and Fe) (Figure 25, top) have been combined with perylene

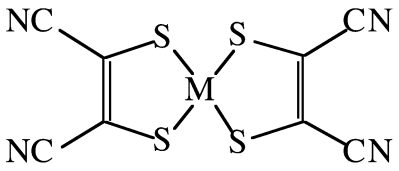

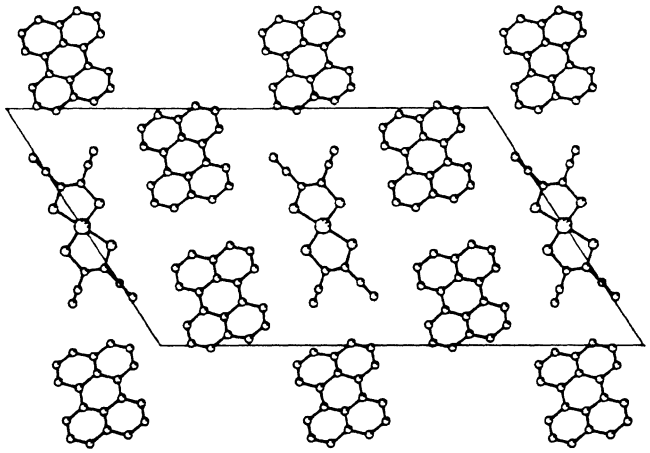

Figure 25. (top) Metal−bismaleonitriledithiolate complexes $[M(mnt)_2]^-$ (M(III) = Ni, Cu, Au, Pt, Pd, Co, and Fe). (bottom) Crystal structure of α-$(Per)_2[M(mnt)_2]$.

(see Chart 1) to form the charge-transfer solids $Per_2M(mnt)_2$. This organic molecule is one of the oldest donors used in the preparation of highly conducting solids. Due to the absence of any chalcogen atoms in the perylene molecule, all known charge-transfer salts based on this donor have a strong one-dimensional character, which is at the origin of the electronic instabilities exhibited by these salts. This feature contrasts with the two-dimensional layered structures adopted by the BEDT-TTF derivatives. A review that discusses the different perylene based compounds can be found in ref 113.

The structures and properties of the $Per_2M(mnt)_2$ salts are summarized in Table 5. They are all

Table 5. Structures and Physical Properties of Perylene Charge-Transfer Salts

compound	packing	electrical properties	magnetic properties	ref
α-$Per_2Pt(mnt)_2$	segregated stacks of perylene and $[Pt(mnt)_2]^-$ complexes; lattice distortion (tetramerization of the perylene chain and dimerization of the inorganic chain) below the metal-to-insulator (M−I) transition	metallic behavior along the stacking axis ($\sigma_{RT} = 700$ S·cm^{-1}); M−I transition at $T_c = 8.2$ K	AF interactions between the spins $S = 1/2$ of the $[Pt(mnt)_2]^-$ units ($J \sim -10$ cm^{-1}); χ vanishes below T_c	114, 115
α-$Per_2Pd(mnt)_2$	same as Pt salt	metallic behavior along the stacking axis ($\sigma_{RT} = 300$ S·cm^{-1}); M−I transition at $T_c = 28$ K	AF interactions between the spins $S = 1/2$ of the $[Pd(mnt)_2]^-$ units ($J \sim -50$ cm^{-1}); χ vanishes below T_c	113
α-$Per_2Ni(mnt)_2$	same as Pt salt	metallic behavior along the stacking axis ($\sigma_{RT} = 700$ S·cm^{-1}); M−I transition at $T_c = 25$ K	AF interactions between the spins $S = 1/2$ of the $[Ni(mnt)_2]^-$ units ($J \sim -100$ cm^{-1}); χ vanishes below T_c	116, 117
α-$Per_2Fe(mnt)_2$	segregated stacks of perylene and $[M(mnt)_2]^-$ complexes; lattice distortion (tetramerization of the perylene chain) observed below the metal-to-insulator transition	metallic behavior along the stacking axis ($\sigma_{RT} = 200$ S·cm^{-1}); M−I transition at $T_c = 58$ K	AF interactions between the spins $S = 3/2$ of the $[Fe(mnt)_2]^-$ units ($J \sim -150$ cm^{-1})	113
α-$Per_2M(mnt)_2$; M = Au, Cu, Co	same as Fe salt	metallic behavior along the stacking axis ($\sigma_{RT} = 700$ S·cm^{-1} for Au and Cu; 200 S·cm^{-1} for Co); M−I transition at $T_c =$ 12.2 K (Au), 32 K (Cu), and 73 K (Co)	weak Pauli paramagnetism that vanishes below T_c	115, 116, 117
β-$Per_2M(mnt)_2$; M = Ni, Cu	segregated stacks of perylene and $[Pd(mnt)_2]^-$ complexes; structural disorder in the perylene chains	semiconductors with ($\sigma_{RT} = 50$ S·cm^{-1})	larger susceptibility than the α-phases; χ follows a $T^{-\alpha}$ law with $\alpha =$ 0.75 (Ni) and 0.8 (Cu) that suggests random exchange AF interactions in the perylene chains	116, 117

essentially isostructural and show similar lattice parameters and diffraction patterns. In several cases (at least for M = Ni, Cu, and Au), the crystals have been obtained in two distinct crystallographic forms denoted as α and β. The structure consists of segregated stacks of perylene and $[M(mnt)_2]^-$ complexes running along the *b*-axis. In the α-phase each stack of $[M(mnt)_2]^-$ is surrounded by six stacks of perylene molecules (Figure 25, bottom). The structure of the β-phase is probably similar, although a full structural refinement does not exist due to the presence of structural disorder.

From the electronic point of view, the α-phase produced the first examples of one-dimensional molecular metals where delocalized electron chains coexist with chains of localized spins. In this respect, some of the properties of these compounds resemble those of Cu(Pc)I, a case where, as we have mentioned earlier, the delocalized electrons belonging to the Pc chain interact with the paramagnetic Cu(II) ions. The properties of those derivatives containing the paramagnetic metal complexes (M = Ni, Pd and Pt, and Fe) are listed in Table 5 and compared with those of derivatives containing diamagnetic metal complexes (M = Au, Cu, and Co). The α-compounds are highly conductive along the stacking axis *b* (∼700 S·cm^{-1} for M = Au, Pt, Ni, and Cu; ∼300 S·cm^{-1} for M = Pd; and ∼200 S·cm^{-1} for M = Fe and Co derivatives), showing a metallic regime at higher temperatures. They undergo metal-to-insulator (M−I) transitions at lower temperatures associated with a tetramerization of the conducting perylene chains ($2k_F$ Peierls transition) (Figure 26a). It is important to emphasize that the magnetic character of the $[M(mnt)_2]^-$ chain does not affect the transport properties and the M−I transition occurs in the same way, irrespective of the paramagnetic or diamagnetic nature of the metal complex.

As far as the magnetic properties are concerned, those compounds with $S = 1/2$ $[M(mnt)_2]^-$ units (M = Pt, Pd, and Ni) undergo a spin−Peierls dimerization of the localized spin chains at the same critical temperature where the M−I transition of the perylene chain takes place. Such a dimerization can be followed by the magnetic susceptibility. Thus, at temperatures well above the transition, the susceptibility indicates antiferromagnetic exchange interactions within the chains with exchange constants of −15, −75, and −150 K for Pt, Pd, and Ni derivatives, respectively. This paramagnetic contribution vanishes at the M−I transition (Figure 26b). The fact that a similar M−I transition also occurs in compounds with diamagnetic $[M(mnt)_2]^-$ units indicates that the Peierls instability in the perylene chain is

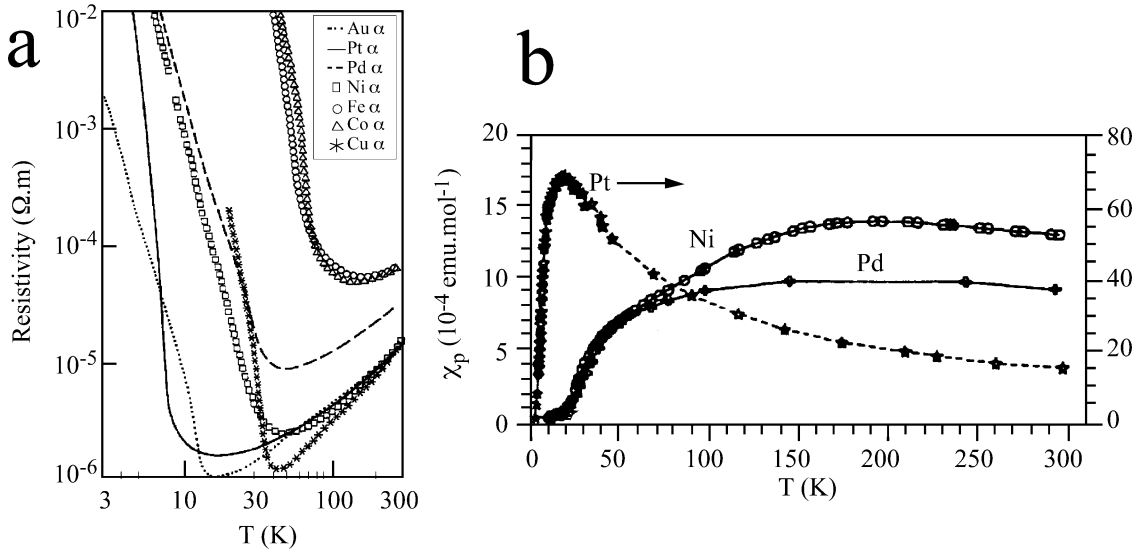

Figure 26. Transport and magnetic properties of the α-$(Per)_2[M(mnt)_2]$ (M(III) = Ni, Pt, Pd) hybrids. (Reprinted with permission from ref 113. Copyright 1997 Wiley.)

the dominant one and the that spin−Peierls transition in the dithiolate chain is triggered by the perylene chain distortion. The existence of an electronic coupling between the two kinds of chains is still controversial. Clearly, the above picture does not require the presence of any exchange interaction between the itinerant electrons and the localized spins, since the structural distortion in the perylene chains can be sufficient to induce the dimerization in the dithiolate chains. However, there are features in the EPR spectra that suggest the presence of fast spin exchange between the two sublattices.[114] An additional insight is provided by the proton NMR spin−lattice relaxation time in the Au and Pt compounds, which is indicative of a coupling of the proton spins of the perylene molecules to the localized spin in the Pt compound.[115]

The β-compounds containing the diamagnetic Cu complex and the paramagnetic Ni complex have also been reported.[116] Both are semiconductors with an electrical conductivity at room temperature in the range 50−80 $S\cdot cm^{-1}$, that is relatively high for semiconductors. They exhibit a significantly larger magnetic susceptibility than the α-phases. Independently of the magnetic character of the metal complexes, both follow a $T^{-\alpha}$ behavior with $\alpha < 1$, which is typical of a random exchange antiferromagnetic chain. This similarity suggests that the structural disorder of this phase is essentially associated with the perylene cations.[117]

4. Ferromagnetic Conductors

So far we have seen that it is possible to make a variety of magnetic charge-transfer salts with discrete or chain inorganic anions that can behave as superconductors and metals, although many such compounds are semiconductors. But, in general, their magnetic properties are not of great interest because they behave as paramagnets down to very low temperatures due to the lack of extended interactions between the metal centers in two or three dimensions. A convenient way to obtain long-range magnetic order is to self-assemble in the hybrid material bimetallic layer anions of the type $[M(II)M(III)(C_2O_4)_3]^-$ (M(II) = Mn, Co, Ni, Fe, Cu; M(III) = Fe, Cr) which behave as ferro- or ferrimagnets with T_c's in the range 5.5−43 K. However, the formation of this bimetallic M(II)M(III) lattice, using as templating cation an organic donor, competes with the formation of the A(I)M(III) lattice, where $A^+ = H_3O$ or a group 1 cation, which has been shown to produce the series of paramagnetic superconductors reported in section 2.1. Thus, synthetic approaches in the absence of these A cations have to be used to reach this goal.

The first step toward building such an array produced a salt containing alternating layers of TTF and a trinuclear anion containing a central Mn(II) with *trans*-oxalate-bridges to two Cr(III) (Figure 27). The salt $(TTF)_4\{Mn(H_2O)_2[Cr(C_2O_4)_3]_2\}\cdot 14H_2O$ contains strongly dimerized TTF^+ and hence is not metallic. This compound exhibits an unprecedented packing in the TTF layer similar to a κ-phase, although the interdimer distances are different in the two directions. Its magnetic susceptibility is nicely fitted by a Heisenberg exchange model for a linear trimer with ferromagnetic Mn(II)−Cr(III) interactions.[118] Quite similar compounds occur for all the combinations of M^{II} = Mn, Fe, Co, Ni, Cu; M^{III} = Cr, Fe.[119] These materials are semiconductors and exhibit either ferromagnetic or antiferromagnetic interactions within the bimetallic trimers, leading to high spin ground states. But, due to the discrete nature of these species, no long magnetic ordering has been observed (Table 6).

The goal of creating a magnetically ordered array between the BEDT-TTF layers has been achieved by the synthesis of a BEDT-TTF salt containing both Mn(II) and Cr(III) in a 2D oxalate-bridged layer. The compound β-$(BEDT\text{-}TTF)_3[MnCr(C_2O_4)_3]$[120] has a structure related to the paramagnetic superconductors reported in section 2.1, but with Mn(II) replacing H_3O^+ within the honeycomb anion layer and only highly disordered small solvent molecules inside the hexagonal cavities (Figure 28). The inorganic layers show an eclipsed stacking with respect to each other. The BEDT-TTF layers adopt a typical

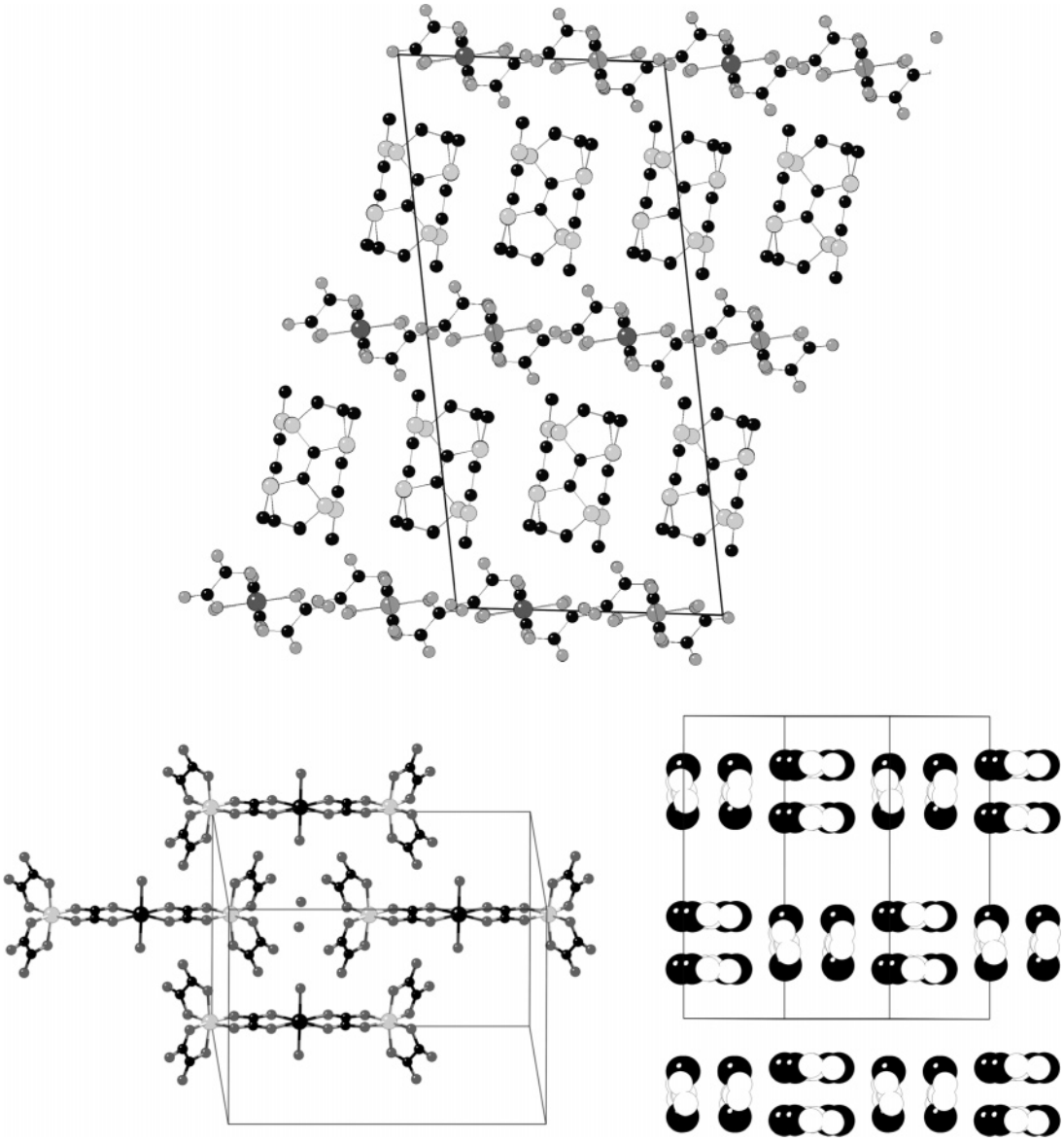

Figure 27. Structure of the radical salts $(TTF)_4\{M^{II}(H_2O)_2[M^{III}(C_2O_4)_3]_2\}\cdot 14H_2O$ (M^{II} = Mn, Fe, Co, Ni, Cu; M^{III} = Cr, Fe) showing the unprecedented pseudo-1D κ-packing in the TTF layer and the presence in the inorganic layer of linear trimer bimetallic oxalato complexes.

regular β-phase arrangement with only one BEDT-TTF molecule in the asymmetric unit. Very short S−S contacts exist between 1D stacks (≈3.4 Å). Recent X-ray data in a bimetallic Mn(II)Rh(III) derivative have revealed the incommensurate nature of these crystals,[121] where both networks do not match, trying to impose their own rigidity. Therefore, the actual stoichiometry of this salt is close to 2.7:1, not 3:1, and the individual charge on the BEDT-TTF molecules must be close to +0.40. Unfortunately, the detailed structural relation between both subsystems has not been found yet.

Having two-dimensionally infinite layers of Mn and Cr bridged by oxalate ions, the compound behaves as a ferromagnet, with T_c of 5.5 K (Figure 29 top), similar to $A[MnCr(C_2O_4)_3]$ salts were A is a tetraalkylammonium cation.[14] The saturation magnetization and coercive field are also similar (Figure 29, center), although in this case the interlayer separation is almost twice, indicating that the magnetic order in such systems has a 2D origin. In dramatic contrast to the latter, however, which are insulators, the BEDT-TTF salt is a metallic conductor, remaining so down to 0.2 K without becoming superconducting (Figure 29, bottom). It remains to be seen to what extent the properties of this remarkable compound can be modified by further tuning of the lattice through varying the metal ions or generating structures containing other donor packing arrangements more commonly associated with superconductivity in BEDT-TTF salts. Several new conducting molecular magnets with either $[MnCr(C_2O_4)_3]^-$ or $[CoCr(C_2O_4)_3]^-$ layers have also been prepared with different TTF derivatives, including the selenium substituted BEST-TTF and BEDT-TSF.[122] A summary of these compounds is reported in Table 6. Magnetically, the change of Mn by Co has raised the T_c up to 9−10 K in these systems. From the conductivity point of view, insulating, semiconducting, and metallic behaviors have been observed, depending on the different packing of the organic donors. In addition to β-packing, α-packings have also been found, such as in the

Table 6. Structures and Physical Properties of Charge-Transfer Salts Containing Bimetallic Oxalate-Bridged Anion Complexes

compound	packing	electrical properties	magnetic properties	ref
$ET_3[MCr(C_2O_4)_3]\cdot CH_2Cl_2$; M = Mn^{II}, Co^{II}	layers of donors (β-packing), and polymeric layers of bimetallic xalate-bridged complexes	metals (σ_{RT} = 250 S·cm^{-1} (MnCr)[a] and 10 S·cm^{-1} (CoCr)[b]); in (CoCr) charge localization below ** K	ferromagnetic (T_c = 5.5 K (MnCr) and 9.2 K (CoCr))	120, 122
$BEST_2[MCr(C_2O_4)_3]\cdot CH_2Cl_2$; M = Mn^{II}, Co^{II}	packing of donors unknown; polymeric layers of bimetallic oxalate-bridged complexes	insulator[b]	ferromagnetic (T_c = 5.6 K (MnCr) and 10.8 K (CoCr))	122
$BETS_3[MnCr(C_2O_4)_3]\cdot CH_2Cl_2$	layers of donors (α-packing), and polymeric layers of bimetallic xalate-bridged complexes	metal (σ_{RT} = 1 S·cm^{-1});[a] charge localization below 150 K	ferromagnetic (T_c = 5.5 K)	123
$BET_3[MCr(C_2O_4)_3]\cdot CH_2Cl_2$; M = Mn^{II}, Co^{II}	packing of donors unknown; polymeric layers of bimetallic oxalate-bridged complexes	metal (σ_{RT} = 21 S·cm^{-1});[b] charge localization below 200 K	ferromagnetic (T_c = 5.5 K (MnCr) and 13.0 K (CoCr))	122
$BEDO_3[MnCr(C_2O_4)_3]\cdot CH_2Cl_2$	packing of donors unknown; polymeric layers of bimetallic oxalate-bridged complexes	metal (σ_{RT} = 1.4 S·cm^{-1});[b] charge localization below 250 K	ferromagnetic (T_c = 5.5 K)	122
$ET_x[MnRh(C_2O_4)_3]\cdot CH_2Cl_2$; x = 2.526(1)	layers of donors (β-packing), and polymeric layers of bimetallic xalate-bridged complexes	metal (σ_{RT} = 13 S·cm^{-1});[a] charge localization below 100 K	paramagnetic	121
$TTF_4\{M(H_2O)_2[M'(C_2O_4)_3]_2\}\cdot nH_2O$; M = Mn^{II}, Fe^{II}, Co^{II}, Ni^{II}, Cu^{II}; M′ = Cr^{III}, Fe^{III}	layers of donors (1D pseudo-κ-packing), and layers of bimetallic oxalate-bridged trimeric complexes	insulator[b]	ferromagnetic coupling (M′ = Cr); antiferromagnetic coupling (M′ = Fe)	118, 119

[a] Measurements on single crystals. [b] Measurements on pressed pellets.

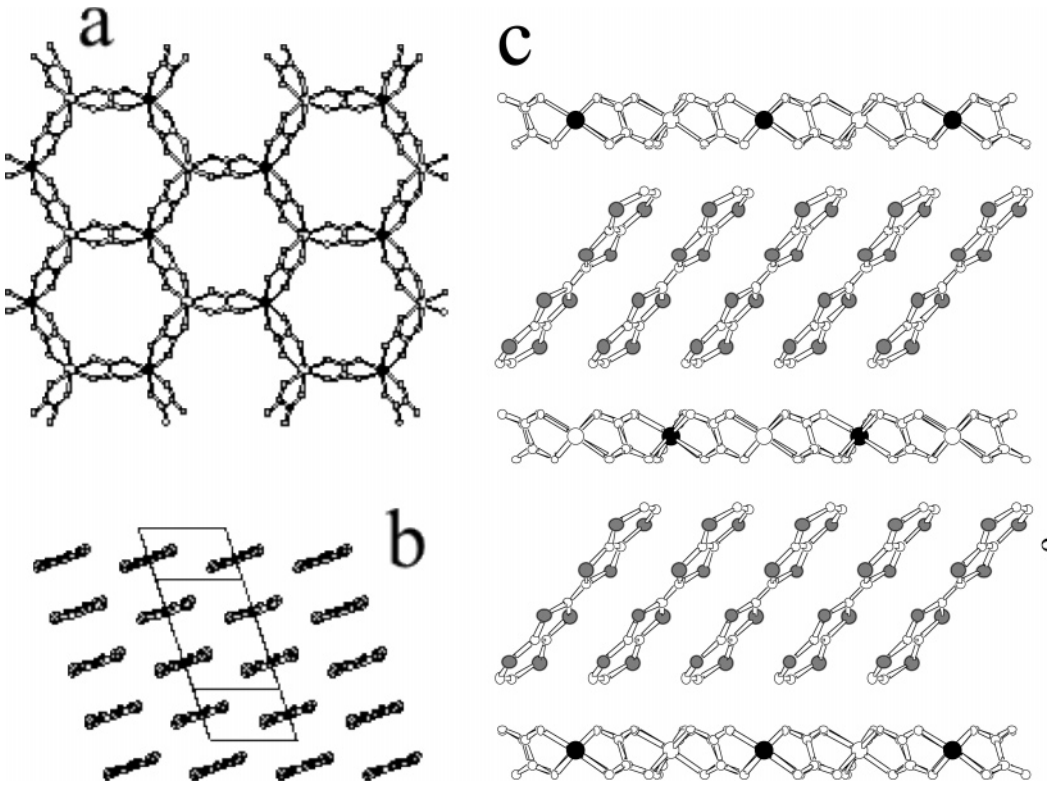

Figure 28. Packing of (a) the $[MnCr(C_2O_4)_3]^-$ anion layer, (b) the BEDT-TTF layer, and (c) the organic and inorganic layers in $(BEDT\text{-}TTF)_3[MnCr(C_2O_4)_3]$. (Reprinted with permission from *Nature* (http://www.nature.com), ref 120. Copyright 2000 Nature Publishing Group.)

salt α-$[BETS]_3[MnCr(C_2O_4)_3]$, which also shows metallic behavior at room temperature but semiconducting behavior below 150 K due to charge localization. No superconducting regime has been detected even at very low temperatures, which keeps open the question of whether the presence of magnetic ordering is responsible for destroying a possible superconducting state. Other factors could be relevant in this regard, such as the structural incommensurability of these phases.

5. Ferrimagnetic Insulators

In previous sections it has been shown that combination of electric with magnetic properties can be

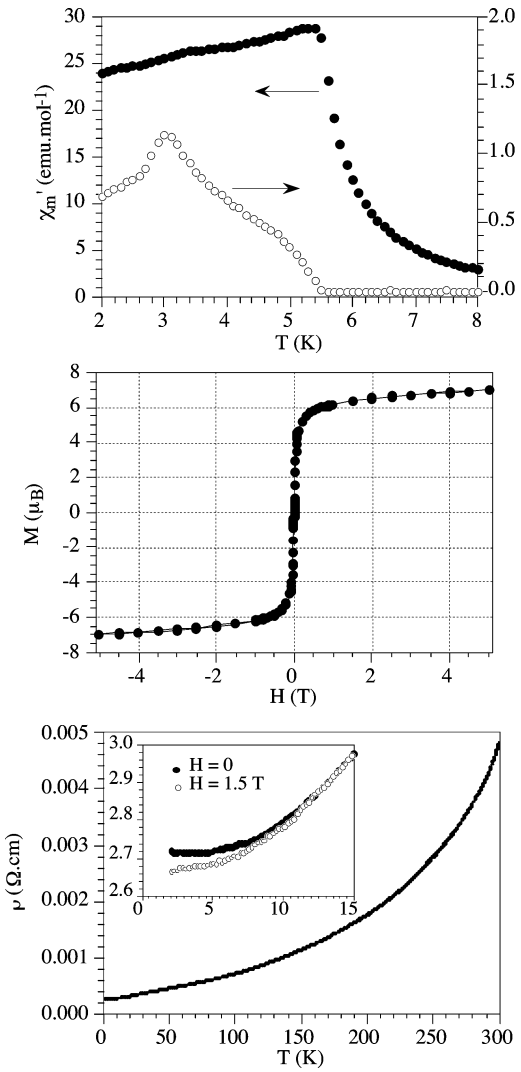

Figure 29. Transport and magnetic properties of the $(BEDT\text{-}TTF)_3[MnCr(C_2O_4)_3]$ showing the coexistence of metallic conductivity and ferromagnetism. (Reprinted with permission from *Nature* (http://www.nature.com), ref 120. Copyright 2000 Nature Publishing Group.)

achieved in two-network materials. Since the contacts between these two networks are of the van der Waals type, the electronic interactions between them remain very weak. For the same reason, within the inorganic magnetic network, the interactions are also very weak, and in most cases, they behave as paramagnets. Thus, cooperative ferromagnetic properties have only been observed when the inorganic network is formed by a 2D extended lattice. Another possibility to reach this goal consists of making the interactions between the two networks strong enough, via $\pi-\pi$ or covalent cation−anion interactions.

One example of this kind is provided by the charge-transfer salts based on partially substituted pseudohalide complexes, of which the Reinecke's anion *trans*-$[Cr(NCS)_4(NH_3)_2]^-$ is a prototype. The salt of Reinecke's anion itself, $(BEDT\text{-}TTF)_2^-[Cr(NCS)_4(NH_3)_2]$, which contains alternating layers of $(BEDT\text{-}TTF)_2^+$ and anions, has magnetic properties dominated by the latter[89] but again no transition to long-range magnetic order above 2 K, despite the presence of several cation−anion S···S contacts less that 4 Å. When the NH_3 is replaced with an aromatic amine, however, the situation is transformed, because, in favorable cases, the planar amines form stacks with the donor cations, in addition to the S···S cation−anion contacts. Under those circumstances, bulk ferrimagnetic order is established: the first such case in charge-transfer salts.

That $\pi-\pi$ cation−anion stacking is important for observing bulk magnetic order in this class of compound is demonstrated in a negative sense by the example of $(BEDT\text{-}TTF)_2[Cr(NCS)_4(2,2'\text{-bipyrimidine})]\cdot 0.25H_2O$. Despite containing an aromatic amine, the structure does not have any π-stacking of the cations and anions, although S···S cation−anion contacts are present.[124] It is paramagnetic down to 2 K, with a very small Weiss constant (−0.26 K).

The first ferrimagnetic charge-transfer salts with a donor pπ and an anion 3d sublattice were based on the Reinecke's anions with isoquinoline (C_9H_7N) as the base.[125] In this case the anion $[M(NCS)_4(C_9H_7N)_2]^-$ (with M = Cr or Fe) has the *trans*-configuration. Charge-transfer salts with 1:1 stoichiometry are formed with BEDT-TTF (M = Cr, Fe) and TTF (M = Cr), the bulk magnetic properties in every instance being classically those of a ferrimagnet, showing full long-range order below a critical temperature T_c. The temperature dependence of $\chi_m T$ has a shallow minimum decreasing from a room temperature value close to that of donor spin $S_D = {}^1/_2$ and anion $S_A = {}^3/_2$ (for Cr^{3+}). Below the minimum, $\chi_m T$ rises rapidly toward saturation at T_c, after which χ_m remains constant so that $\chi_m T$ decreases linearly. Below T_c the isothermal magnetization saturates at 2 Nμ_B for the Cr salt, corresponding to an antiferromagnetic alignment between S_A and S_D; there is also

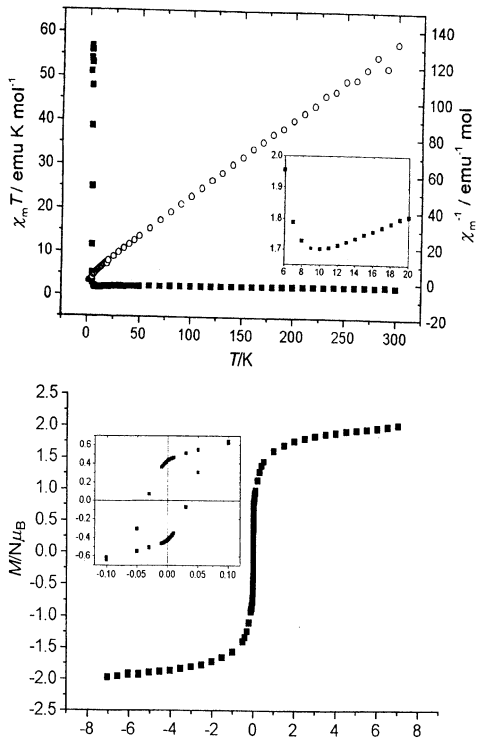

Figure 30. Magnetic data for the ferrimagnetic salt $(BEDT\text{-}TTF)[Cr(NCS)_4(C_9H_7N)_2]$: (top) $\chi_m T$ (filled squares) and χ_m^{-1} versus temperature T (the inset shows the minimum in $\chi_m T$ at 10 K); (bottom) magnetization versus field (the inset shows the hysteresis).

Table 7. Magnetic Parameters for Ferrimagnetic Charge-Transfer Salts D[M(NCS)$_4$B$_2$][a]

	I	II	III	IV
T_c/K	4.2	8.9	4.5	9.0
$\chi_m T$ (at 330 K)/emu·K·mol^{-1}	2.26	2.18	4.75	2.22
minimum $\chi_m T$/emu·K·mol^{-1}	1.7	0.99	3.97	1.2
minimum T/K	9.9	16.9	14.8	17.5
coercive field/Oe	338	75	18	~0
remanent M/Nμ_B	0.42	0.74	0.38	~0
M_{sat} at 7 T/Nμ_B	2.0	2.1	4.3	1.7

[a] I: D = BEDT-TTF; M = Cr; B = C_9H_7N; ref 125. II: D = TTF; M = Cr; B = C_9H_7N; ref 125. III: D = BEDT-TTF; M = Fe; B = C_9H_7N; ref 125. IV: D = TTF; M = Cr; B = phen; ref 126.

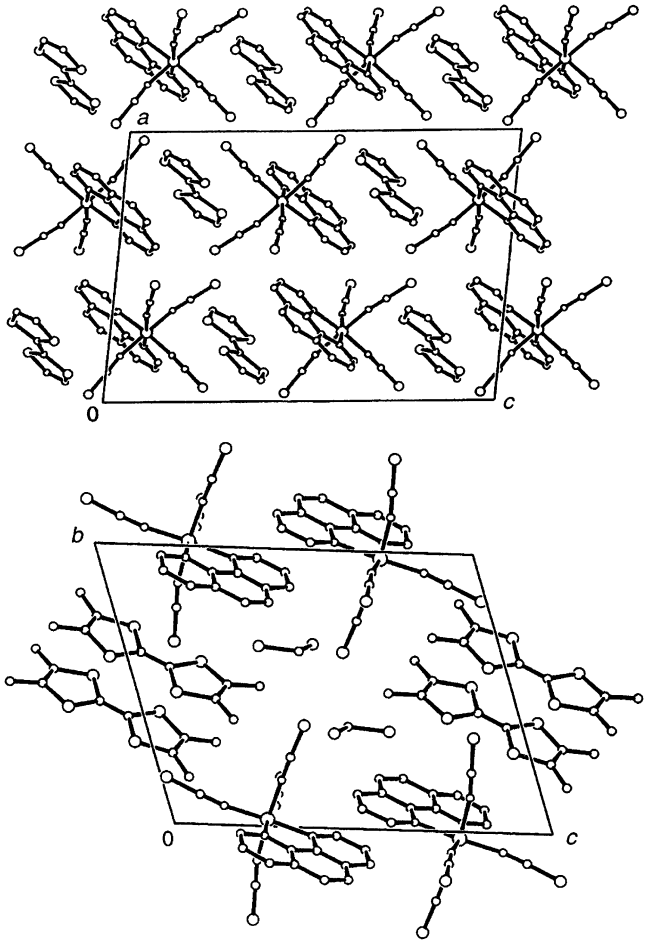

Figure 31. Crystal structures of (a) (TTF)[Cr(NCS)$_4$phen] and (b) (TMTTF)[Cr(NCS)$_4$phen].

a modest hysteresis. Typical magnetic data for these compounds are shown in Figure 30, and the magnetic parameters are listed in Table 7.

When isoquinoline is replaced by 1,10-phenanthroline, the anion necessarily has the *cis*-configuration, but TTF, TMTTF, and TMTSF salts have also been obtained.[126] The TTF salt of [Cr(NCS)$_4$phen]$^-$ is a ferrimagnetic insulator with T_c = 9 K (IV in Table 7), while the TMTTF salt is an antiferromagnetic insulator (T_N = 3 K). In both compounds there are close intermolecular contacts between the phenanthroline and the donor as well as S···S contacts between the cations and anions. The difference in the bulk magnetic properties appears to be the result of the larger steric requirement of TMTTF, because the latter salt consists of dimerized cations while in the TTF one there are stacks of alternating cations and anions (Figure 31). The π-interaction between cations and anions is also disrupted in the TMTTF compound compared to the TTF one (Figure 32).[127]

The important role played by the cation−anion $\pi-\pi$ overlap in determining the collective magnetic properties in this class of compounds is confirmed by synthesizing a large number of salts of general type D[M(NCS)$_n$L$_m$], where D is an organo-chalcogen donor, M is Cr^{3+} or Fe^{3+}, and L is an aromatic ligand such as isoquinoline, phen, or their substituted derivatives. Among the dozen or so such salts known (see Tables 3 and 7), only the ones containing L, and where the crystal structure indicates D···L $\pi-\pi$ overlap, behave as long-range-ordered ferrimagnets at low temperature.[128] Some salient magnetic parameters for those compounds are listed in Table 7. In a few cases magnetic hysteresis has been observed, while EPR directly confirms the presence of an internal field in the ordered state by a substantial apparent shift in the observed g-value below T_N.[129,130]

6. Conclusions

It is clear from this review that compounds containing electron donor molecules of the kind that form molecular metals and superconductors can be synthesized with a wide variety of transition metal-containing anions, which introduce localized magnetic moments into the lattice. Correspondingly, while many of these contain alternating layers consisting of cations and anions alone, they are formed

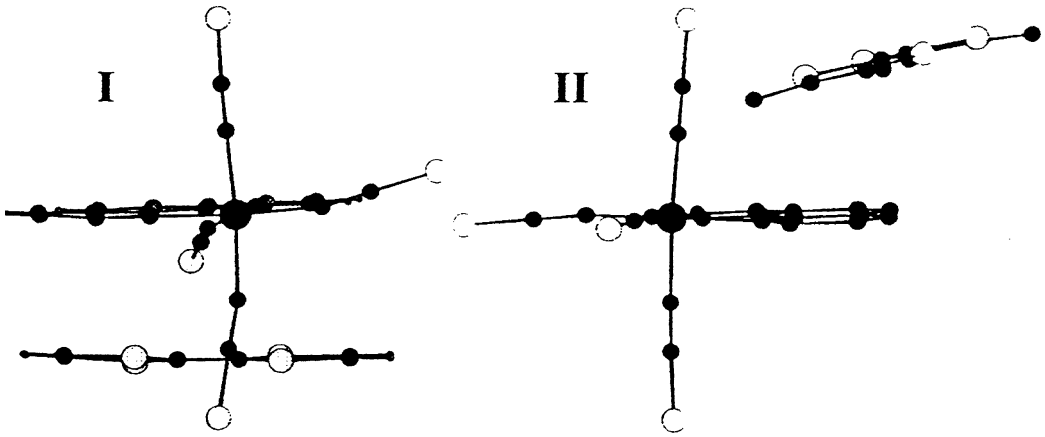

Figure 32. Cation−anion $\pi-\pi$ stacking in A[Cr(NCS)$_4$phen]: I, A = TTF; II, A = TMTTF.

with many different packing motifs of the donor cations. Insulators, semiconductors, metals, and superconductors are all represented. Examples also exist where the anions interact with the cations through weak H-bonds, S···S contacts shorter than the van der Waals distance, or $\pi\cdots\pi$ stacking contacts. Nevertheless, in the large majority of cases it is fair to say that experimental evidence for exchange interactions between donor π and metal d electrons, or metal d electrons via a delocalized donor π system, is difficult to identify conclusively. Exceptions are $(BEDT\text{-}TTF)_3CuBr_4$[68] and κ-$(BETS)_2FeCl_4$,[38,39] but the change in conductivity of the latter when the Fe(III) moments order antiferromagnetically might also be due to magnetostriction. While it is possible, too, that the failure of the metallic compound $(BEDT\text{-}TTF)_3[MnCr(C_2O_4)_3]$ to become superconducting at low temperature may be the result of ferromagnetic order in the anion layer, there is no unambiguous evidence that this is the case.[120] It is true that in those salts where S···S and $\pi\cdots\pi$ stacking interactions occur between cations and anions, transitions to long-range ferrimagnetic order occur, with one sublattice being furnished by the cation π orbitals and the other by the anion d orbitals. However, in that case the interactions are strong enough to break up the donor cation layers and, since cations and anions are interdigitated, the resulting compounds are semiconductors or insulators. Nevertheless, a rich harvest of novel molecular materials has emerged, such as paramagnetic and antiferromagnetic superconductors, a ferromagnetic metal, and ferromagnetic semiconductors. No doubt, further synthetic ingenuity will uncover more novelty in the future.

7. Acknowledgment

Financial support of the Spanish Ministerio de Ciencia y Tecnología (Grant MAT-3507) and the European Union (TMR Network on Molecular Magnetism: From Materials to Devices) is acknowledged. The writing of this article was greatly facilitated by discussions with partners within the EC COST D14 003/99 Action. P.D. thanks the IBERDROLA Foundation for a Visiting Professorship at the University of Valencia, during which this review was written. He is also grateful to colleagues at the University of Valencia for their warm welcome.

8. References

(1) Day, P. *Philos. Trans. R. Soc. London* **1985**, *A314*, 140.
(2) Coronado, E.; Galán-Mascarós, J. R.; Giménez-Saiz, C.; Gómez-Garcia, C. J In *Magnetism: A Supramolecular Function*; Kahn, O., Ed.; NATO ASI Series C484; Kluwer Academic Publishers: The Netherlands, 1996; pp 281−298 and references therein.
(3) (a) Matsubara, T.; Kotani, A. *Superconductivity in Magnetic and Exotic Materials*; Springer Series in Solid State Scienc; Springer: Berlin, 1984; Vol. 52; pp 1−211. (b) Jensen, M. A.; Suhl, H. In ref 3a, p 183.
(4) (a) Elliott, J. R. In *Magnetism*; Rado, Suhl, Eds.; Academic Press: New York, 1965; Vol. IIA, p 385. (b) Mott, N. F. *Metal−Insulator Transitions*; Taylor & Francis: London, 1990. (c) For a detailed description of the exchange interactions in molecular materials, including the RKKY one, see also: Coronado, E.; Georges, R.; Tsukerblat, B. In *Molecular Magnetism. From Molecular Assemblies to the Devices*; Coronado, E., Delhaes, P., Gatteschi, D., Miller, J. S., Eds.; NATO ASI Series E321; Kluwer Academic Publishers: The Netherlands, 1996; p 65.
(5) Ginzburg, V. L. *Sov. Phys. JETP* **1957**, *4*, 153.
(6) Matthias, B. T.; Suhl, M.; Corenzwit, E. *Phys. Rev. Lett.* **1959**, *1*, 92.
(7) Fertig, W. A.; Johnson, D. C.; Delong, L. E.; McCallum, R. W.; Maple, M. B.; Matthias, B. T. *Phys. Rev. Lett.* **1977**, *38,* 987.
(8) Ishikawa, M.; Fischer, Ø. *Solid State Commun.* **1977**, *23,* 37.
(9) Moncton, D. E.; McWhan, D. B.; Schmidt, R. H.; Shirane, G.; Thomlinson, W.; Maple, M. B.; McKay, H. B.; Woolf, L. D.; Fisk, Z.; Johnston, D. C *Phys. Rev. Lett.* **1980**, *45,* 2060.
(10) Lynn, J. W.; Shirane, G.; Thomlinson, W.; Shelton, R. N.; Moncton, D. E. *Phys. Rev.* **1981**, *B24,* 3817.
(11) Bernhard, C.; Tallon, J. L.; Niedermayer, Ch.; Blasins, Th.; Golnik, A.; Brucher, E.; Kremer, R. H.; Noakes, D. R.; Stronach, C. E.; Ansaldo, E. J. *Phys. Rev. B* **1999**, *59,* 14099.
(12) Ishikawa, M.; Fischer, Ø. *Solid State Commun.* **1977**, *24,* 747.
(13) Hamaker, H. C.; Woolf, I. D.; McKay, H. B.; Fisk, Z.; Maple, M. B. *Solid State Commun.* **1979**, *32,* 289.
(14) Tamaki, H.; Zhong, Z. J.; Matsamoto, N.; Kida, S.; Koikawa, M.; Achiwa, N.; Hashimoto, Y.; Okawa, H. *J. Am. Chem. Soc.* **1992**, *114,* 6974.
(15) Mathionière, C.; Carling, S. G.; Dou, Y.; Day, P. *J. Chem. Soc., Chem. Commun.* **1994**, 1551.
(16) Kurmoo, M.; Graham, A. W.; Day, P.; Coles, S. J.; Hursthouse, M. B.; Caulfield, J. M.; Singleton, J.; Ducasse, L.; Guionneau, P. *J. Am. Chem. Soc.* **1995**, *117,* 12209.
(17) (a) Martin, L. L.; Turner, S. S.; Day, P.; Guionneau, P.; Howard, J. A. K.; Hibbs, D. E.; Light, M. E.; Hursthouse, M. B.; Uruichi, M.; Yakushi, K. *Inorg. Chem* **2001**, *40,* 1363. (b) Martin, L. L.; Turner, S. S.; Day, P.; Mabbs, F. E.; McInnes, E. J. L. *J. Chem. Soc., Chem. Commun.* **1997**, 1367.
(18) Turner, S. S.; Day, P.; Malik, K. M. A.; Hursthouse, M. B.; Tent, S. J.; MacLean, E. J.; Martin, L. L *Inorg. Chem.* **1999**, *38*, 3543.
(19) Rashid, S.; Turner, S. S.; Le Pevelen, D.; Day, P.; Light, M. E.; Hursthouse, M. B.; Firth, S.; Clark, R. J. H. *Inorg. Chem.* **2001**, *40,* 5304.
(20) Graham, A. W.; Kurmoo, M.; Day, P. *J. Chem. Soc., Chem. Commun.* **1995**, 2061.
(21) Yamochi, H.; Komatsu, T.; Matsukawa, N.; Saito, G.; Mori, T.; Kusunoki, M.; Sakagushi, K. *J. Am. Chem. Soc.* **1993**, *155*, 11319.
(22) Coronado, E.; Clemente-León, M.; Galán-Mascarós, J. R.; Giménez-Saiz, C.; Gómez-García, C. J.; Martínez-Ferrero, E. *J. Cluster Sci.* **2002**, *13*, 381.
(23) Kurmoo, M.; Talham, D.; Day, P.; Parker, I. D.; Friend, R. H.; Stringer, A. M.; Howard, J. A. K. *Solid State Commun.* **1987**, *61,* 459.
(24) Rosseinsky, M. J.; Kurmoo, M.; Talham, D.; Day, P.; Chasseau, D.; Watkin, D. *J. Chem. Soc., Chem. Commun.* **1988**, 88.
(25) Rashid, S.; Turner, S. S.; Day, P.; Howard, J. A. K.; Guinonneau, P.; McInnes, E. J. L.; Mabbs, F. E.; Clark, R. J. H.; Firth, S.; Biggs, T. *J. Mater. Chem.* **2001**, *11*, 2095.
(26) Narduzzo, A.; Ardavan, A.; Coldea, A. I.; Singleton, J.; Akutsu-Sato, A.; Akutsu, H.; Turner, S. S.; Day, P. *Synth. Met.* **2003**, *137*, 1225.
(27) Kobayashi, H.; Tomita, H.; Naito, T.; Kobayashi, A.; Sakai, F.; Watanabe, T.; Cassoux, P. *J. Am. Chem. Soc.* **1996**, *118*, 368.
(28) Goze, F.; Laukhin, V. N.; Brossard, L.; Audonard, A.; Ulmet, J. P.; Askenazy, S.; Naito, T.; Kobayashi, H.; Kobayashi, A.; Tokumoto, M.; Cassoux, P. *Physica* **1995**, *B211,* 290.
(29) Brossard, L.; Clerac, R.; Coulon, C.; Tokumoto, M.; Ziman, T.; Petrov, D. K.; Laukhin, V. N.; Naughton, M. J.; Audonard, A.; Goze, F.; Kobayashi, A.; Kobayashi, H. *Eur. Phys. J.* **1998**, *Bl*, 439.
(30) Tamaka, H.; Adachi, T.; Ojima, E.; Fujiwara, H.; Kato, K.; Kobayashi, H.; Kobayashi, A.; Cassoux, P. *J. Am. Chem. Soc.* **1999**, *121*, 11243.
(31) Sato, A.; Ojima, E.; Kobayashi, H.; Hoshkoshi, Y.; Inose, K.; Kobayashi, A.; Cassoux, P. *Adv. Mater* **1999**, *11*, 1192.
(32) Uji, S.; Shinagawa, H.; Tereshima, T.; Yakabe, T.; Terai, Y.; Tokumoto, M.; Kobayashi, A.; Tanaka, H.; Kobayashi, H. *Nature* **2001**, *410*, 908.
(33) Balicus, L.; Brooks, J. S.; Storr, K.; Uji, S.; Tokumoto, M.; Kobayashi, H.; Kobayashi, A.; Tanaka, H.; Burzykin, V.; Gorkov, L. P. *Phys. Rev. Lett.* **2001**, *87*, 067002.
(34) Brooks, J. S.; Balicas, L.; Storr, K. A.; Kobayashi, H.; Tanaka, H.; Kobayashi, A.; Uji, S.; Tokumoto, M. *Synth. Met.* **2003**, *133−134,* 485.
(35) Kobayashi, H.; Tanaka, H.; Fujiwara, H.; Tamura, I.; Gritsenko, V.; Otsuka, T.; Fujiwara, E.; Kobayashi, A.; Tokumoto, M.; Cassoux, P. *Synth. Met.* **2003**, *133−134,* 477.
(36) Uji, S.; Terakuar, C.; Terashima, T.; Yakabe, T.; Imanaka, Y.; Yasuzuka, S.; Tokumoto, M.; Sakai, F.; Kobayashi, A.; Tanaka, H.; Kobayashi, H.; Balicas, L.; Brooks, J. S. *Synth. Met.* **2003**, *133−134,* 481.
(37) (a) Meul, H. W.; Rossel, C.; Decroux, M.; Fischer, O.; Remenyi, G.; Briggs, A. *Phys. Rev. Lett.* **1984**, *53,* 497. (b) Cepas, O.; Merino, J.; McKenzie, R. H. *Phys. Rev.* **2002**, *B65*, 100502.
(38) Ojima, E.; Fujiwara, H.; Kato, K.; Kobayashi, H.; Tanaka, H.; Kobayashi, A.; Tokumoto, M.; Cassoux, P. *J. Am. Chem. Soc.* **1999**, *121*, 5581.

(39) Fujiwara, H.; Kobayashi, H.; Fujiwara, E.; Kobayashi, A. *J. Am. Chem. Soc.* **2002**, *124,* 6816. See also: Otsuka, T.; Cui, H. B.; Fujiwara, H.; Kobayashi, H.; Fujiwara, E.; Kobayashi, A. *J. Mater. Chem.* **2004**, *14*, 1682.
(40) Zhang, B.; Tanaka, H.; Fujiwara, H.; Kobayashi, H.; Fujiwara, E.; Kobayashi, A. *J. Am. Chem. Soc.* **2002,** *124*, 9982.
(41) Ogawa, M. Y.; Hoffmann, B. M.; Lee, S.; Yudkowsky, M.; Halperin, W. P. *Phys. Rev. Lett.* **1986**, *57*, 1177.
(42) (a) Caron, L. G.; Bourbonnais, C. *Synth. Met.* **1994**, *41*−*43*, 3941. (b) Yainakado, H.; Ida, T.; Ugawa, A.; Yakushi, K.; Awaga, K.; Maruyama, Y.; Imaeda, K.; Inokuchi, H. *Synth. Met.* **1994**, *62*, 169.
(43) Bechgaard, K.; Carneiro, K.; Rasmassen, F. G.; Olsen, K.; Rindorf, G.; Jacobsen, C. S.; Pederson, H. J.; Scott, J. E. *J. Am. Chem. Soc.* **1981**, *103*, 2240.
(44) Batail, P.; Ouahab, L.; Torrance, J. B.; Pylman, M. L.; Parkin, S. S. P. *Solid State Commun.* **1985**, *55*, 597.
(45) Batail, P.; Ouahab, L. *Mol. Cryst. Liq. Cryst.* **1985**, *125***,** 205.
(46) Kumai, R.; Asamitsu, A.; Tokura, Y. *Chem. Lett.* **1996**, 753; *Synth. Met.* **1997**, *85*, 1681.
(47) Mallah, T.; Hollis, C.; Bott, S.; Kurmoo, M.; Day, P. *J. Chem. Soc., Dalton Trans.* **1990**, 859.
(48) Beno, M. A.; Cox, D. D.; Williams, J. M.; Kwak, J. F. *Acta Crystallogr.* **1984**, *C40*, 1334.
(49) Kobayashi, H.; Kato, R.; Mori, T.; Kobayashi, A.; Sasaki, Y.; Saito, G.; Inokuchi, H. *Chem. Lett.* **1983**, 759.
(50) Kobayashi, H.; Mori, T.; Kato, R.; Kobayashi, A.; Sasaki, Y.; Saito, G.; Inokuchi, H. *Chem. Lett.* **1983**, 581.
(51) Leung, P. C. W.; Beno, M. A.; Blackman, G. S.; Coughlin, B. R.; Midenski, C. A.; Joss, W.; Crabtree, G. W.; Williams, J. M. *Acta Crystallogr.* **1984**, *C40*, 1331.
(52) Kurmoo, M.; Talham, D.; Day, P.; Howard, J. A. K.; Stringer, A.; Parker, I.; Obertelli, A.; Friend, R. H. *Synth. Met.* **1988**, *22*, 415.
(53) Kurmoo, M.; Day, P.; Guionneau, P.; Gaultier, J.; Chasseau, D.; Ducasse, L.; Allen, M. L.; Marsden, I. D.; Bravic, G.; Friend, R. H. *Inorg. Chem.* **1996**, *35*, 4719.
(54) Ayllon, J. A.; Santos, I. C.; Henriques, R. T.; Almeida, M.; Lopes, E. B.; Morgardo, J.; Alcacer, L.; Veiros, L. F.; Durante, M. T. *J. Chem. Soc., Dalton Trans.* **1995**, 3543.
(55) Lequan, M.; Lequan, R. M.; Hauw, C.; Gaultier, J.; Maceno, G.; Delhaes, P. *Synth. Met.* **1987**, *19*, 409.
(56) Garrigou-Lagrange, Ch.; Rozanski, S. A.; Kurmoo, M.; Pratt, F. L.; Maceno, G.; Delhaes, P.; Lequan, M.; Lequan, R. M. *Solid State Commun.* **1988**, *67,* 481.
(57) Lequan, M.; Lequan, R. M.; Mecano, G.; Delhaes, P. *J. Chem. Soc., Chem. Commun.* **1988**, 174.
(58) Mori, T.; Inokuchi, H. *Bull. Chem. Soc. Jpn.* **1988**, *61*, 591.
(59) Mori, T.; Wang, P.; Imaeda, K.; Enoki, T.; Inokuchi, H. *Solid State Commun.* **1987**, *64*, 773.
(60) Sugano, T.; Takenouchi, H.; Chiomi, D.; Kinoshita, M. *Synth. Met.* **1991**, *41*−*43*, 2217.
(61) Coronado, E.; Falvello, L. R.; Galán-Mascarós, J. R.; Giménez-Saiz, C.; Gómez-García, C. J.; Lauhkin, V. N.; Pérez-Benítez, A.; Rovira, C.; Veciana, J. *Adv. Mater.* **1997**, *9*, 984.
(62) (a) Kurmoo, M.; Mallah, T.; Marsden, L.; Allan, M.; Friend, R. H.; Pratt, F. L.; Hayes, W.; Chasseau, D.; Bravic, G.; Duchase, L.; Day, P. *J. Am Chem. Soc.* **1992**, *114*, 10722. (b) Gudenko, A. V.; Ginodman, V. B.; Korotkov, V. E.; Koshelap, A. V.; Kushch, N. D.; Laukhin, V. N.; Rozenberg, L. P.; Khomenko, A. G.; Shibaeva, R. P.; Yagubskii, E. B. In *The Physics and Chemistry of Organic Superconductors*; Saito, G., Kagoshima, G., Eds.; Springer-Verlag: Berlin, Germany, 1990.
(63) Kobayashi, H.; Kato, R.; Mori, T.; Kobayashi, A.; Sasaki, Y.; Saito, G.; Enoki, T.; Inokuchi, H. *Chem. Lett.* **1984**, 179.
(64) Kurmoo, M.; Talham, D. R.; Day, P.; Chasseau, D.; Watkin, D. *J. Chem. Soc., Chem. Commun.* **1988**, 88.
(65) Kurmoo, M.; Mallah, T.; Day, P.; Marsden, I.; Allan, M.; Friend, R. H.; Pratt, F. L.; Hayes, W.; Chasseau, D.; Gaultier, J.; Bravic, G. In *The Physics and Chemistry of Organic Superconductors*; Saito, G., Kagoshima, S., Eds.; Springer-Verlag: New York, 1990; pp 290−293.
(66) Kobayashi, H.; Kato, R.; Mori, T.; Kobayashi, A.; Sasaki, Y.; Saito, G.; Enoki, T.; Inokuchi, H. *Chem. Lett.* **1984**, 179.
(67) Bleaney, B.; Bowers, K. D. *Proc. R. Soc.* **1952**, *A214*, 451.
(68) Marsden, I. R.; Allan, M. L.; Friend, R. H.; Kurmoo, M.; Kanazawa, D.; Day, P.; Bravic, G.; Chasseau, D.; Duchase, L.; Hayes, W. *Phys. Rev.* **1994**, *B50*, 2118.
(69) Guionneau, P.; Bravic, G.; Gaultier, J.; Chasseau, D.; Kurmoo, M.; Kanazawa, D.; Day, P. *Acta Crystallogr*. **1994**, *C50*, 1894.
(70) Guionneau, P.; Gaultier, J.; Chasseau, D.; Bravic, G.; Barrans, Y.; Ducasse, L.; Kanazawa, D.; Day, P.; Kurmoo, M. *J. Phys. I* **1996**, *6*, 1581.
(71) Kurmoo, M.; Kanazawa, D.; Day, P.; Marsden, I. R.; Allen, M. L.; Friend, R. H. *Synth. Met.* **1993**, *55*−*57,* 2347.
(72) Tsuchiya, R.; Yoshizaki, S.; Nakamura, T.; Takahashi, T.; Yamamura, J.; Suzuki, K.; Enoki, T.; Saito, G. *Synth. Met.* **1995**, *70*, 967.
(73) Fitzmaurice, J. C.; Slavin, A. M. C.; Williams, D. J.; Woolins, D. J. *J. Chem. Soc., Chem. Commun.* **1993**, 1479.
(74) Enoki, T.; Yamamura, J.-I.; Sugiyasu, N.; Suzuki, K.; Saito, G. *Mol. Cryst. Liq. Cryst.* **1993**, *233*, 325.
(75) Galamzyanov, A. A.; Ignater, A. A.; Kusch, N. D.; Laukhin, V. N.; Makova, M. K.; Merzhanov, V. A.; Rozenberg, L. P.; Shibaeva, R. P.; Yagubskii, E. B. *Synth. Met.* **1989**, *33*, 81.
(76) Kepert, C. J.; Kurmoo, M.; Day, P. *J. Mater. Chem* **1997**, *7*, 221.
(77) Aldoshira, M. Z.; Veratternikova, L. S.; Lubovskaya , R. N.; Khidekel, M. L. *Transition Met. Chem.* **1980**, *5,* 63.
(78) Bouherour, S.; Ouahab, L.; Pena, O.; Padiou, J.; Grandjean, D. *Acta Crystallogr.* **1989**, *C45*, 371.
(79) Le Magueres, P.; Ouahab, L.; Briard, P.; Even, J.; Bertault, M.; Toupet, L.; Ramos, J.; Gómez-García, C. J.; Delhaes, P. *Mol. Cryst. Liq. Cryst.* **1997**, *305*, 479.
(80) Rahal, M.; Chasseau, D.; Gaultier, J.; Ducasse, L.; Kurmoo, M.; Day, P. *Acta Crystallogr.* **1997**, *B53*, 159.
(81) Clemente-León, M.; Coronado, E.; Galán-Mascarós, J. R.; Giménez-Saiz, C.; Gómez-García, C. J.; Fabre, J. M. *Synth. Met.* **1999**, *103*, 2279.
(82) Clemente-León, M.; Coronado, E.; Galán-Mascarós, J. R.; Giménez-Saiz, C.; Gómez-García, C. J.; Ribera, E.; Vidal-Gancedo, J.; Rovira, C.; Canadell, E.; Lauhkin, V. *Inorg. Chem.* **2001**, *40*, 3526.
(83) Mori, H.; Hirabayashi, I.; Tanaka, S.; Mori, T.; Manyama, Y. *Synth. Met.* **1995**, *70,* 789.
(84) Pratt, F. L.; Singleton, J.; Doporto, M.; Fisher, A. J.; Janssen, T. J. B. M.; Perenboon, J. A. A. J.; Kurmoo, M.; Hayes, W.; Day, P. *Phys. Rev.* **1992**, *B45*, 13904.
(85) Honold, M. M.; Harrison, N.; Nam, M.-S.; Singleton, J.; Mielke, C. H.; Kurmoo, M.; Day, P. *Phys. Rev.* **1998**, *B58*, 1.
(86) Bérézovsky, F. Ph.D. Dissertation, Université de Bretagne Occidentale (France), 2000.
(87) Bérézovsky, F.; Triki, S.; Sala Pala, J.; Galán-Mascarós, J. R.; Gómez-García, C. J.; Coronado, E. *Synth. Met.* **1999**, *102*, 1755.
(88) Thétiot, F.; Bérézovsky, F.; Triki, S.; Sala-Pala, J.; Gómez-García, C. J.; Hajem, A. A.; Bouguessa, S.; Fabre, J. M. *C. R. Chim.* **2003**, *6*, 291.
(89) Turner, S. S.; Day, P.; Gelbrich, T.; Hursthouse, M. B. *J. Solid State Chem.* **2001**, *159*, 385.
(90) Triki, S.: Thétiot, F.; Sala-Pala, J.; Gómez-García, C. J.; Coronado, E. Submitted.
(91) Mas-Torrent, M.; Turner, S. S.; Wurst, K.; Vidal-Gancedo, J.; Veciana, J.; Rovira, C.; Day, P. *Synth. Met.* **2001**, *120*, 799.
(92) (a) Clemente-León, M.; Coronado, E.; Galán-Mascarós, J. R.; Giménez-Saiz, C.; Gómez-García, C. J.; Fabre, J. M. *Synth. Met.* **1999**, *103*, 2279. (b) Coronado, E.; Galán-Mascarós, J. R.; Gómez-García, C. J. *J. Chem. Soc., Dalton Trans.* **2000**, 205.
(93) Rashid, S.; Turner, S. S.; Day, P.; Light, M. E.; Hursthouse, M. B. *Inorg. Chem.* **2000**, *39*, 2426.
(94) Martin, L.; Turner, S. S.; Day, P.; Giuonneau, P.; Howard, J. A. K.; Uriuchi, M.; Yakushi, K. *J. Mater. Chem.* **1999**, *9*, 2731.
(95) (a) Triki, S.; Bérézovsky, F.; Pala, J. S.; Riou, A.; Molinié, P. *Synth. Met.* **1999**, *103*, 1974. (b) Triki, S.; Bérézovsky, F.; Pala, J. S.; Gómez-García, C. J.; Coronado, E.; Costuas, K.; Halet, J. F. *Inorg. Chem.* **2001**, *40*, 5127.
(96) (a) Triki, S.; Bérézovsky, F.; Pala, J. S.; Gómez-García, C. J.; Coronado, E. *J. Phys. IV* **2000**, *10*, 35. (b) Triki, S.; Bérézovsky, F.; Sala-Pala, J.; Riou, A.; Molinié, P. *Synth. Met.* **1999**, *103*, 1974.
(97) Cotton, F. A.; Robinson, W. R.; Walton, R. A.; Whyman, R. *Inorg. Chem.* **1967**, *6*, 929.
(98) Kepert, C. J.; Kurmoo, M.; Day, P. *Inorg. Chem.* **1997**, *36*, 1128.
(99) Robertson, N.; Awaga, K.; Parsons, S.; Kobayashi, A.; Underhill, A. E. *Adv. Mater. Opt. Electron.* **1998**, *8,* 93.
(100) Deplano, P.; Leoni, L.; Mercuri, M. L.; Schlueter, J. A.; Geiser, U.; Wang, H. H.; Kini, A. M.; Manson, J. L.; Gómez-García, C. J.; Coronado, E.; Koo, H. J.; Whangbo, M. H. *J. Mater. Chem.* **2002**, *12*, 3570.
(101) Awaga, K.; Okuno, T.; Maruyama, Y.; Kobayashi, A.; Kobayashi, H.; Schenk, S.; Underhill, A. E. *Inorg. Chem.* **1994**, *33,* 5598.
(102) Takahashi, M.; Takeda, M.; Awaga, K.; Okuno, T.; Maruyama, Y.; Kobayashi, A.; Kobayashi, H.; Schenk, S.; Robertson, N.; Underhill, A. E. *Mol. Cryst. Liq. Cryst.* **1996**, *286*, 77.
(103) Underhill, A. E.; Robertson, N.; Ziegenbalg, J.; Le Narvor, N.; Kilburn, J. D.; Awaga, K. *Mol. Cryst. Liq. Cryst.* **1996**, *284,* 39.
(104) (a) Coronado, E.; Gómez-García, C. J. *Chem. Rev.* **1998**, *98,* 273. (b) Clemente-León, M.; Coronado, E.; Giménez-Saiz, C.; Gómez-García, C. J. In *Polyoxometalate Molecular Science*; Borrás, J. J., Coronado, E., Müller, A., Pope, M. T., Eds.; NATO ASI Series 98: Mathematics, Physics and Chemistry; Kluwer Academic Publishers: Dordrecht, The Netherlands, 2003; pp 417−440.
(105) Davidson, A.; Boubekeur, K.; Pénicaud, A.; Auban, P.; Lenoir, C.; Batail, P.; Hervé, G. *J. Chem. Soc., Chem. Commun.* **1989**, 1372.
(106) (a) Gómez-García, C. J.; Ouahab, L.; Giménez-Saiz, C.; Triki, S.; Coronado, E.; Delhaes, P. *Angew. Chem., Int. Ed. Engl.* **1994**, *33,* 223. (b) Gómez-García, C. J.; Giménez-Saiz, C.; Triki, S.; Coronado, E.; Le Magueres, P.; Ouahab, L.; Ducasse, L.; Sour-

isseau, C.; Delhaes, P. *Inorg. Chem*. **1995**, *34*, 4139. (c) Gómez-García, C. J.; Giménez-Saiz, C.; Triki, S.; Coronado, E.; Ducasse, L.; Le Magueres, P.; Ouahab, L.; Delhaes, P. *Synth. Met*. **1995**, *70*, 783.
(107) (a) Kurmoo, M.; Day, P.; Bellitto, C. *Synth. Met.* **1995**, *70*, 963. (b) Bellitto, C.; Bonamico, M.; Fares, V.; Federici, F.; Righini, G.; Kurmoo, M.; Day, P. *Chem. Mater*. **1995**, *7,* 1475.
(108) (a) Galán-Mascarós, J. R.; Giménez-Saiz, C.; Triki, S.; Gómez-García, C. J.; Coronado, E.; Ouahab, L. *Angew. Chem., Int. Ed. Engl*. **1995**, *34*, 1460. (b) Coronado, E.; Galán-Mascarós, C. J.; Giménez-Saiz, C.; Gómez-García, C. J.; Triki, S.; Delhaes, P. *Mol. Cryst. Liq. Cryst*. **1995**, *274*, 89. (c) Coronado, E.; Galán-Mascarós, J. R.; Giménez-Saiz, C.; Gómez-García, C. J.; Triki, S. *J. Am. Chem. Soc*. **1998**, *120*, 4671.
(109) (a) Coronado, E.; Galán-Mascarós, J. R.; Giménez-Saiz, C.; Gómez-García, C. J.; Laukhin, V. N. *Adv. Mater*. **1996**, *8*, 801. (b) Coronado, E.; Clemente-Leon, M.; Galán-Mascarós, J. R.; Giménez-Saiz, C.; Gómez-García, C. J.; Martínez-Ferrero, E. *J. Chem. Soc., Dalton Trans.* **2000**, 3955. (c) Borrás-Almenar, J. J.; Clemente-Juan, J. M.; Clemente-León, M.; Coronado, E.; Galán-Mascarós, J. R.; Gómez-García, C. J. In *Polyoxometalate chemistry: From topology via self-assembly to applications*; Pope, M. T., Müller, A., Eds.; Kluwer: New York, 2001; pp 231−253.
(110) Gómez-García, C. J.; Borrás-Almenar, J. J.; Coronado, E.; Delhaes, P.; Garrigou-Lagrange, C.; Baker, L. C. W. *Synth. Met.* **1993**, *56*, 2023.
(111) Clemente-León, M.; Coronado, E.; Galán-Mascarós, J. R.; Giménez-Saiz, C.; Gómez-García, C. J.; Fernández-Otero, T. *J. Mater. Chem*. **1998**, *8*, 309.
(112) Clemente-Juan, J. M.; Coronado, E. *Coord. Chem. Rev*. **1999**, *193*−*195*, 361.
(113) Almeida, M.; Henriques, R. T. In *Handbook of Organic Conductive Molecules and Polymers. Volume 1: Charge-transfer salts, Fullerenes and Photoconductors*; Nalwa, H. S., Ed.; John Wiley & Sons Ltd.: New York, 1997; Chapter 2, p 87.
(114) Bourbonnais, C.; Henriques, R. T.; Wzietek, P.; Kongeter, D.; Voiron, J.; Jerome, D. *Phys. Rev.* **1991**, *B44*, 641.
(115) Henriques, R. T.; Alcacer, L.; Almeida, M.; Tomic, S. *Mol. Cryst. Liq. Cryst.* **1985**, *120*, 237.
(116) Gama, V.; Almeida, M.; Henriques, R. T.; Santos, I. C.; Domingos, A.; Ravy, S.; Pouget, J. P. *J. Phys. Chem*. **1991**, *95*, 4263.
(117) Gama, V.; Henriques, R. T.; Almeida, M.; Alcacer, L. *J. Phys. Chem.* **1994**, *98*, 997.
(118) Coronado, E.; Galán-Mascarós, J. R.; Ruiz-Pérez, C.; Triki, S. *Adv. Mater*. **1996**, *8*, 737.
(119) (a) Coronado, E.; Galán-Mascarós, J. R.; Giménez-Saiz, C.; Gómez-García, C. J. *Synth. Met.* **1997**, *85*, 1677. (b) Coronado, E.; Galán-Mascarós, J. R.; Giménez-Saiz, C.; Gómez-García, C. J.; Ruiz-Pérez, C. *Eur. J. Inorg. Chem.* **2003**, 2290.
(120) Coronado, E.; Galán-Mascarós, J. R.; Gómez-García, C. J.; Laukhin, V. *Nature* **2000**, *408*, 447.
(121) Coronado, E.; Galán-Mascarós, J. R.; Gómez-García, C. J.; Martínez-Ferrero, E.; Van Smaalen, S. *Inorg. Chem.* **2004**, *43*, 4808.
(122) (a) Alberola, A.; Coronado, E.; Galán-Mascarós, J. R.; Giménez-Saiz, C.; Gómez-García, C. J.; Romero, F. M. *Synth. Met.* **2003**, *133*−*134*, 509. (b) Alberola, A.; Coronado, E.; Galán-Mascarós, J. R.; Giménez-Saiz, C.; Gómez-García, C. J.; Martínez-Ferrero, E.; Murcia-Martínez, A. *Synth. Met.* **2003**, *135*−*136*, 687.
(123) Alberola, A.; Coronado, E.; Galán-Mascarós, J. R.; Giménez-Saiz, C.; Gómez-García, C. *J. Am. Chem. Soc.* **2003**, *125,* 10774.
(124) Kepert, C. J.; Kurmoo, M.; Truter, M. R.; Day, P. *J. Chem. Soc., Dalton Trans.* **1997**, 607.
(125) Turner, S. S.; Michaut, C.; Durot, D.; Day, P.; Gelbrich, T.; Hursthouse, M. B. *J. Chem. Soc., Dalton Trans.* **2000**, 905.
(126) Turner, S. S.; Le Pevelen, D.; Day, P.; Prout, K. *J. Chem. Soc., Dalton Trans.* **2000**, 2739.
(127) Le Pevelen, D.; Turner, S. S.; Day, P.; Prout, K. *Synth. Met*. **2001**, *120*, 1842.
(128) Turner, S. S.; Le Pevelen, D.; Day, P. *Synth. Met.* **2003**, *133,* 497.
(129) Mas-Torrent, M.; Turner, S. S.; Wurst, K.; Vidal-Gancedo, J.; Ribas, X.; Veciana, J.; Day, P.; Rovira, C. *Inorg. Chem.* **2003**, *42*, 7544.
(130) Ouahab, L.; Enoki, T. *Eur. J. Inorg. Chem.* **2004**, 933.

CR030641N